HHS Public Access

Author manuscript

*Dev Biol*. Author manuscript; available in PMC 2021 February 01.

Published in final edited form as:

*Dev Biol*. 2020 February 01; 458(1): 12–31. doi:10.1016/j.ydbio.2019.10.005.

# Insights into intestinal regeneration signaling mechanisms

**Samir A. Bello**, **Vanessa Torres-Gutiérrez**, **Eneric J. Rodríguez-Flores**, **Ernesto J. Toledo-Román**, **Natalia Rodríguez**, **Lymarie M. Díaz-Díaz**, **Lionel D. Vázquez-Figueroa**, **José M. Cuesta**, **Valentina Grillo-Alvarado**, **Alexandra Amador**, **Josean Reyes**, **José E. García-Arrarás**

Department of Biology, University of Puerto Rico, Rio Piedras Campus, San Juan, PR

## Abstract

The cellular mechanisms underlying the amazing ability of sea cucumbers to regenerate their autotomized intestines have been widely described by us and others. However, the signaling pathways that control these mechanisms are unknown. Previous studies have shown that Wnt homologs are upregulated during early intestinal regenerative stages, suggesting that the Wnt/β-catenin pathway is active during this process. Here, we used small molecules, putative disruptors of the *Wnt* pathway, to determine the potential role of the canonical Wnt pathway on intestine regeneration in the sea cucumber *Holothuria glaberrima*. We evaluated their effects *in vivo* by using histological analyses for cell dedifferentiation, cell proliferation and apoptosis. We found that iCRT14, an alleged Wnt pathway inhibitor, decreased the size of the regenerating intestine, while LiCl, a presumed Wnt pathway activator, increased its size. The possible cellular mechanisms by which signaling pathway disruptors affect the gut rudiment size were further studied *in vitro*, using cultures of tissue explants and additional pharmacological agents. Among the tested signaling modulators that act through GSK-3 inhibition, LiCl, 1-Azakenpaullone, and CHIR99021 were found to increase muscle cell dedifferentiation, while iCRT14 blocked cell dedifferentiation. Differently, cell proliferation was reduced by all GSK-3 inhibitors, as well as by iCRT14 and C59, which interferes with Wnt ligand secretion. The *in vivo* temporal and spatial pattern of β-catenin activity was determined using an antibody against phosphorylated β-catenin and shown to correlate with cell proliferative activity. *In vitro* treatment using C59 decreased the number of cells immunostained for nuclear phosphorylated β-catenin. Our results showed that the cell dedifferentiation observed during intestinal regeneration can be decoupled from the cell proliferation event and that these cellular events can be modulated by particular signaling pathway inhibitors and activators. These results open the door for future studies where the cellular signaling pathways involved at each regeneration stage can be determined.



**Conflict of interest:** The authors declare that they have no conflicts of interest with the contents of this article.

**Keywords**

Wnt/β-catenin; GSK-3 inhibitors; sea cucumber; intestine regeneration; muscle dedifferentiation; cell proliferation

## Introduction

Regenerative phenomena are common in echinoderms, a group of invertebrate deuterostomes. Among them, holothurians or sea cucumbers are able to rapidly regenerate their digestive tract after their spontaneous or induced ejection (Hyman, 1955; García-Arrarás et al., 1998). Our laboratory has extensively studied the cellular events underlying intestinal regeneration in an echinoderm model: the sea cucumber *Holothuria glaberrima* (García-Arrarás et al., 1998; Mashanov and García-Arrarás, 2011). In this species, following evisceration, a new intestine is formed from the free end of the remaining mesentery. The main cell source for the new intestine is the outer tissue layers of the mesentery, the mesothelium, which is made up of peritoneocytes (or coelomic epithelia) and muscle cells. These cells dedifferentiate during early stages of intestine regeneration giving rise to progenitor-like cells. The dedifferentiation process in muscle cells can be followed as the cells condense their myofilaments into membrane bound spindle-like structures (SLSs) (Dolmatov and Ginanova, 2001). Thus, SLSs are the hallmark of muscle dedifferentiation in echinoderms (Candelaria et al., 2006; García-Arrarás and Dolmatov, 2010). Dedifferentiated cells regain their ability to proliferate during intestine regeneration and, later on, these cells re-differentiate and form the mesothelium of the new intestine (Murray and García-Arrarás, 2004). A transient increase in programmed cell death in the gut rudiment mesothelium has also been documented at early regeneration stages, suggesting that apoptosis, in addition to dedifferentiation and cell proliferation, is also involved in holothurian intestine regeneration (Mashanov et al., 2010).

Although the cellular events associated with intestine regeneration in sea cucumbers have been spatially and temporally described, there is a gap in knowledge about the signaling mechanisms that control them. Previous molecular studies, from our group and others, have provided correlative evidence for a role of Wnt family members. First, a Wnt-9 homolog was shown to be upregulated during the first week of intestinal regeneration (Ortiz-Pineda et al., 2009). Similar findings, focusing on Wnt-4, Wnt-6, Wnt-7, frizzled-7, and dishevelled homologs in sea cucumbers of the species *Apostichopus japonicus* (Sun et al., 2013; Yuan et al., 2019) and WntA, Wnt-4, and Wnt-6, frizzled-1/2/7, and frizzled-4 homologs in sea cucumbers of the species *Eupenctacta fraudatrix* (Girich et al., 2017), were shown at early stages of intestine regeneration. Second, *in situ* hybridization studies demonstrated that Wnt-9 transcripts are highly expressed in the mesothelial cells of the regenerating holoturian intestine from early stages of regeneration (Mashanov et al., 2012). Wnt homolog upregulation coincides spatiotemporally with the key cellular events occurring during intestine regeneration, suggesting that these events might be under the control of Wnt signaling pathways.

The Wnt protein family consists of secreted glycoproteins that have crucial roles in the regulation of many biological processes through activation of different signaling pathways (Komiya and Habas, 2008; Whyte et al., 2012; Clevers and Nusse, 2012). Among the signaling pathways modulated by Wnts is the canonical or Wnt/β-catenin dependent pathway. The canonical Wnt pathway is characterized by the stabilization and accumulation of β-catenin protein in the cytoplasm and its subsequent localization in the nucleus after Wnt ligand binding (on-state) to the receptor complex (frizzled receptor and LRP5/6 co-receptors). In the nucleus, β-catenin binds to transcription factors, acting as a transcriptional co-activator of target genes. In the absence of Wnt ligands (off-state), β-catenin is targeted for degradation by the proteasome following its phosphorylation by Glycogen Synthase Kinase-3 (GSK-3), a key component of the β-catenin destruction complex, resulting in reduced levels of nuclear β-catenin. The expression of Wnt ligands and antagonists is tightly regulated spatiotemporally leading to Wnt signaling activation or inhibition at specific times and localizations during development, homeostasis and regeneration (Komiya and Habas, 2008).

GSK-3 is a serine/threonine protein kinase that originally received its name due to its ability to phosphorylate the enzyme glycogen synthase, a key regulator of glycogen metabolism. It is widely accepted that GSK-3 regulates multiple cellular functions, among them are many metabolic and signaling pathways. Mammals possess two GSK-3 isoforms, GSK-3α and GSK-3β (Cormier and Woodgett, 2017). In non-vertebrates, only one GSK-3 homolog has been described to date, except in Planarians, where three isoforms have been identified (Adell et al., 2008).

The possibility that Wnt is involved in the process of intestinal regeneration is not surprising since accumulating evidence support a key role of the canonical Wnt pathway during organ or tissue regeneration in various animal systems. Wnt/β-catenin signaling disruption in animals with strong regenerative abilities results in impairment of regeneration (Whyte et al., 2012). For example Wnt is involved in apical regeneration in Hydra (Chera et al., 2009), head regeneration in Planaria (Gurley et al., 2008) and fin regeneration in zebrafish (Stoick-Cooper et al., 2007) among others. In recent years, data have been accumulating indicating that the Wnt signaling pathway is much more complex than previously thought. In this respect Wnt/β-catenin activation of cellular processes has been shown to occur in some cases in a GSK-3 independent manner (Devotta et al., 2018) and contrariwise, some cellular processes have been shown to be modulated by GSK-3 in a manner independent of Wnt/β-catenin (Jope and Johnson, 2004).

Small cell-permeant molecules, which include the GSK-3 inhibitors, have been used to modulate the canonical Wnt signaling pathway in some regeneration models (Gonsalves et al., 2011). Here, we have used several of these small-permeant molecules *in vivo* and *in vitro* (Table 1 and Table S1) to determine their effect on intestinal regeneration in *H. glaberrima*. Our results suggest that, while the Wnt/β-catenin pathway might be involved in regulating cellular proliferation, the muscle dedifferentiation is modulated by a GSK-3 dependent, Wnt-independent mechanism.

## Materials and Methods

### Animal collection and evisceration

Adult sea cucumbers (*Holothuria glaberrima)* were collected from the rocky shores of northeastern Puerto Rico. Upon arrival to the laboratory, animals were injected with 3 mL of 0.35M KCl into the coelomic cavity to induce evisceration. A diagram illustrating visceral anatomy before and after evisceration is shown in Fig. 1A–B. Following evisceration they were maintained in indoor seawater aquaria at room temperature (RT, 20–24°C) with constant aeration. Animals were anesthetized by immersion in 0.2 % 1,1,1-trichloro-2-methyl-2-propanol hemihydrate (chlorobutanol, Sigma) in natural sea water for 20–30 min before sacrificed (4–10 days post-evisceration (dpe)).

## In vivo studies

### Pharmacological treatment

Sea cucumbers were injected intracoelomically with the putative Wnt signaling antagonist iCRT14 or the putative agonist lithium chloride (LiCl). For iCRT14 treatment, animals were injected daily with 40 mg per kg of animal weight for days 1–7, with a final injection at 10 dpe (Fig. 2A, red arrows). The volume of stock solution (25 mg/mL) containing the amount of iCRT14 required per animal was mixed with natural sea water to complete a final volume of 300 μL injected into each animal. Control animals were injected with the same volume (300 μL) of DMSO (vehicle) diluted in natural sea water. For LiCl treatment, sea cucumbers were injected daily for 8 days with 1 ml of 140 mM LiCl solubilized in milliQ water (Fig. 2E, red arrows). The volume of coelomic fluid per animal is approximately 7 ml; therefore, the final concentration of LiCl in the coelomic fluid has been estimated to be approximately 20 mM. Control animals were injected with 1 ml of 140 mM sodium chloride (NaCl) solubilized in milliQ water. To determine cell proliferation, iCRT14-treated animals were injected with two pulses of bromodeoxyuridine (BrdU, 50 mg per kg of animal weight). The first BrdU pulse was co-injected with the iCRT14 at 7 dpe, and the second pulse was co-injected with the iCRT14 at 10 dpe (Fig 2A, black arrows). LiCl-treated animals were injected with a single pulse of BrdU (50 mg per kg of animal weight) 18–24h before being sacrificed at 10 dpe (Fig. 2E, black arrow). Animals were sacrificed at 10 or 11 dpe. Before dissection, the anterior-posterior length of each animal was measured. Then, a segment comprising the third quarter (from anterior to posterior length) of the body wall and attached mesentery and gut rudiment were dissected out (as shown in Fig. 1B–C) and processed for immunohistochemical studies. In this manner, we used only a posterior segment of the gut rudiment for histological studies. LiCl, NaCl, iCRT14, and BrdU were purchased from Sigma-Aldrich.

### Immunohistochemistry

Gut rudiments were fixed in 4% paraformaldehyde (PFA) in 0.1M phosphate buffered saline (PBS) overnight at 4°C. After fixation, tissues were rinsed thrice with PBS (15 min each) and cryoprotected in 30% sucrose/PBS at 4°C. Gut rudiments were mounted in OCT compound (Sakura, Finetek, USA) and cryosectioned (20 μm) using a Leica CM1850 cryostat. Immunohistochemical staining for BrdU incorporation detection was performed as

previously described (García-Arrarás et al., 2011). Briefly, tissue sections were permeabilized with 1% Triton X-100 for 15 min, followed by two washes with PBS. Then, slides were treated with 0.05M HCl for 1h. After an additional wash with PBS, the tissues were blocked with normal goat serum. Then the slides were incubated with the primary antibody anti-BrdU (1:5, GE Healthcare RPN202) overnight. Next day, the slides were washed three times with PBS for 15 min each wash. Then, the tissue sections were incubated with the secondary antibody goat anti-mouse labeled with Cy3 (GAM-Cy3, 1:1,000, Jackson Immuno Research Laboratories) for an hour at room temperature. After three additional washes with PBS, slides were mounted in buffered glycerol solution containing 1 μg/ml of 4',6-diamidino-2-phenylindole (DAPI, Sigma). Finally, tissue sections were visualized and analyzed using a Nikon Eclipse Ni fluorescence microscope.

Muscle and spindle-like structures were detected in tissue sections using Phalloidin-TRITC staining (1:1,000, Sigma P1951). Slides were incubated with diluted Phalloidin for one hour, then washed three times with PBS and mounted in buffered glycerol solution containing DAPI (García-Arrarás et al., 2011).

We used a monoclonal anti-mouse β-catenin antibody that specifically recognizes β-catenin when phosphorylated on Tyr 489 (PY489-β-catenin) to localize the protein in tissue sections of regenerating intestines in *H. glaberrima*. We obtained the PY489-β-catenin antibody as supernatant (Lot Number 7/2/15–15μg/ml) and by growing PY489-β-catenin cells (Lot Number 2/16/16) from the Developmental Studies Hybridoma Bank, University of Iowa. The supernatant was added to fresh tissue sections without any previous treatment, and then incubated overnight. Next day, we followed the same protocol used for the secondary antibody staining (GAM-Cy3, 1:1,000, Jackson Immuno Research Laboratories) as explained above.

Drug effects on gut rudiment size, SLSs distribution in the mesentery, cell proliferation, apoptosis, and β-catenin expression were evaluated in at least three animals as biological replicates (n = 3) using three to five non-consecutive tissue sections per animal, as explained below.

### Gut rudiment area

Gut rudiment photographs were taken using the Nikon DS-Q12 digital camera. Gut rudiment area was measured on photographs using the Image J software (http://rsbweb.nih.gov/ij/). At least four non- consecutive tissue sections were evaluated to obtain the average of gut rudiment area per animal.

### Muscle dedifferentiation

We used a semiquantitative system described previously by our group (Pasten et al., 2012) to evaluate the degree of muscle dedifferentiation *in vivo*. As previously stated, SLSs are a hallmark of muscle dedifferentiation in sea cucumbers (Candelaria et al., 2006). As intestine regeneration advances, mesenterial muscle dedifferentiates in a gradient; first, dedifferentiation is observed at the free edge of the mesentery and, as regeneration proceeds, it advances toward the body wall. This can be seen as the gradual disappearance of muscle fibers paired with the appearance of SLSs. Consequently, the system used to evaluate the

muscle dedifferentiation takes into account the localization of the SLSs in the mesentery relative to the gut rudiment and the body wall, assigning a score according to the distances of the SLSs to the rudiment and the body wall. Score ranges from 0, where the SLSs are present in the gut rudiment, to 5 where the SLS are only observed adjacent to the body wall. At least three non-consecutive tissue sections were used to evaluate the degree of muscle dedifferentiation per animal.

### Cell proliferation

The percentage of BrdU labeled cells was calculated in at least two non-consecutive intestine tissue sections (from three different regions of the gut rudiment) of iCRT14 or LiCl treated animals by counting BrdU labeled cells and DAPI labeled nuclei in micrographs taken with 40× objective (area = 85,580 $\mu m^2$) and imported to Image J software. The percentage of BrdU labeled cells in each region was calculated and averaged to obtain the percent of BrdU labeled cells per animal. DAPI is a nuclear dye that labels all nuclei, thus providing the number of total cells within the field of view so as to obtain the percentage of total cells labeled by the BrdU.

### Apoptosis

Apoptosis was quantified by terminal deoxynucleotidyl transferase dUTP nick end labeling (TUNEL) using the FragEl DNA fragmentation detection kit (Calbiochem, QIA39) on cryosections of iCRT14 and LiCl treated animals and their respective controls. The cryosections were processed for TUNEL assays following the protocol provided by the manufacturers. Briefly, the tissues were permeabilized for 5 min using proteinase K, and then incubated with equilibration buffer at room temperature for 15 min. Subsequently, they were incubated with a mixture of fluorescently labeled and unlabeled deoxynucleotides and the terminal deoxynucleotidyl transferase enzyme for 1.5 hours at 37°C in a wet chamber. The tissue sections were mounted using the Fluorescein-FragEl mounting media containing 1 μg/ml of DAPI. Finally, tissue sections were visualized and analyzed using a Nikon Eclipse Ni fluorescence microscope. The percentage of TUNEL labeled cells was calculated in at least two non- consecutive tissue sections (from three different regions of the gut rudiment) of iCRT14 or LiCl treated animals by counting TUNEL labeled cells and DAPI labeled nuclei in micrographs taken with 40× objective and imported to Image J software. The percentage of TUNEL labeled cells in each region was calculated and averaged to obtain the percent of TUNEL labeled cells per animal.

### Nuclear β-catenin staining

The percentage of PY489-β-catenin labeled cells was calculated in two non-consecutive tissue sections in normal (non-eviscerated) mesentery (at three different regions: distal, medial, and proximal mesentery), in normal intestines, and in regenerating intestines at 3, 7, and 14 dpe (at three different regions of the gut rudiment) by counting PY489-β-catenin labeled nuclei and DAPI labeled nuclei per field of view in micrographs taken with 40× objective and imported to Image J software. The percentage of PY489-β-catenin labeled cells in each region was calculated and averaged to obtain the percent of PY489-β-catenin labeled cells per animal.

## In vitro studies

### Cell culture

Gut rudiments with their associated mesenteries were dissected from sea cucumbers at 4 dpe. Gut rudiment explants were surface disinfected as described previously (Bello et al., 2015) and carefully placed in 24-well plates, one explant per well. Each explant was covered with 1 mL of Leibovitz-15 cell culture medium (L-15) conditioned for marine species (Schacher and Proshansky, 1983) and supplemented with antibiotics (100 U/mL penicillin, 100 μg/mL streptomycin, 50 μg/mL gentamicin), antifungal (2.5 μg/mL amphotericin B), 1× MEM nonessential amino acids, 1 mM sodium pyruvate, 1.75 μg/mL α-tocopherol acetate, and 1× ITS (Insulin, Transferrin, and Sodium Selenite). All cell culture reagents were purchased from Sigma-Aldrich. Explants were incubated in a modular incubator chamber (Billups-Rothenberg Inc) at room temperature (20–24°C).

### Pharmacological treatment of explants

Intestine explants dissected at 4 dpe were treated with small molecules that have been used as Wnt pathway modulators (agonists or antagonists) in other models, as shown in Table 1 and Table S1. Presumed Wnt agonists evaluated were: LiCl (20 mM), 1-Azakenpaullone (100, 20, and 2 μM), CHIR99021 (20, and 5 μM), and SKL2001 (a.k.a. Wnt agonist II) (200, 50, and 5 μM). Putative Wnt antagonists tested were: iCRT14 (50 μM), EGCG (500, 150, and 50 μM), C59 (15, 5, and 1 μM), and XAV939 (100, 50, and 15 μM). The drug doses were chosen based on studies of Wnt modulation performed on other model systems. LiCl and EGCG were solubilized in milliQ- water and the remaining drugs were solubilized in DMSO. Stock solutions were added to the culture medium to obtain the final concentrations mentioned above. LiCl and EGCG control explant groups were treated with NaCl and milliQ-water, respectively. NaCl was added to increase the concentration by 20 mM in control explants. For the remaining groups, we used 0.2–0.5% DMSO for controls. C59 and XAV939 were purchased from Cellagen Technology. The rest of drugs were purchased from Sigma-Aldrich. Explants were grown in 1 mL of culture medium in 24-well plates with small molecules for 48–72h. Medium was changed after 24 and 48h. To determine the effect of the pharmacological agents on cell proliferation, 50 μM BrdU was added to the culture medium 24h before fixation of explants.

We also performed a dose-response experiment where gut explants dissected at 14 dpe were treated with different doses (2, 10, and 20 mM) of LiCl while control explants were treated with the same concentrations of NaCl. Explants were treated for 48h with 1 mL of the cell culture medium containing LiCl or NaCl. Culture medium was changed after 24h. At this point, 50 μM BrdU was added to the culture medium to determine the effect of LiCl on cell proliferation.

### Histological and Immunohistochemical analyses

Explants were fixed in 4% PFA and processed for histological and immunohistochemical analyses as explained above for *in vivo* tissues. SLSs/DAPI ratio, cell proliferation, apoptosis, and nuclear β-catenin staining were evaluated in at least three explants, each explant from one animal (n=3) using two to three tissue sections per animal.

### Muscle dedifferentiation

The number of SLSs and DAPI labeled nuclei per field of view were manually counted under the fluorescence microscope using the 100× objective (area = 13,837 $\mu m^2$) for each tissue section on three different regions of the mesentery: near the gut rudiment, medial segment, and near the body wall (Fig. 7B). The number of SLSs and cell nuclei in the three regions was averaged to obtain the SLSs/DAPI ratio per tissue section. At least two non-consecutive tissue sections were used per explant.

### Cell proliferation, apoptosis and nuclear β-catenin staining

The percentage of BrdU, TUNEL, and PY489-β-catenin labeled cells in explants was determined as explained above for *in vivo* tissues with a modification. The main difference was that the counting *in vitro* was performed in photographs taken in both the gut rudiment and the mesentery (in three regions: distal, medial, and proximal mesentery) of explants. Conversely, the counting in *in vivo* studies was focused on photographs taken in different regions within the gut rudiment.

The data obtained in experiments performed *in vivo* and *in vitro* to determine the effect of Wnt pathway modulators on gut rudiment size, cell proliferation (% of BrdU positive cells), and apoptosis (% of TUNEL positive cells) were normalized by dividing each value from the biological replicates by the mean value from the control group, to report the effect of treatments as fold changes. Thus, a two-fold increase in the experimental group average data compared to control group (for example gut rudiment size in $\mu m^2$), means that the average value in treated group is twice the value observed in the control group.

### Statistical analyses

For evaluation of statistical differences between control and experimental groups, we employed an unpaired t-test or one-way ANOVA followed by Tukey's test or Dunnett's tests. Welch's correction was applied to data when the assumption of homogeneity of variance was not accomplished. These analyses were performed using the software GraphPad Prism 5. All values are reported as mean ± standard deviation (SD).

## Results

### 1. Wnt signaling pathway modulators modify the gut rudiment size

The initial goal of these experiments was to determine a possible role of the Wnt canonical signaling pathway in intestinal regeneration. To achieve this goal, eviscerated sea cucumbers were injected daily during one week with either the putative Wnt inhibitor (iCRT14) (Fig. 2A) or the putative Wnt activator (LiCl) (Fig. 2E). Controls were injected with DMSO or NaCl, respectively. The mesenteries with the regenerating intestines were dissected out and processed for histological studies at 10–11 dpe (Figs. 2A & 2E). Animals at this stage have formed an intestinal rudiment at the distal tip of the mesentery, and some of them have already formed a lumen. The rudiment is a solid rod of tissue that extends from the esophagus to the cloaca and, when sectioned transversally, shows a rounded, tear-shaped morphology (Fig. 2B). We observed that both iCRT14 (Fig. 2B) and LiCl (Fig. 2F) treatments had an effect on the size of the regenerating gut rudiment when compared to

those of control treated animals (Figs. 2C & 2G). When the area of the gut rudiment from iCRT14-treated animals was compared with controls, it was significantly smaller (about 50%) (Fig. 2D). Moreover, we found that none of the iCRT14-treated animals (n = 9) exhibited gut rudiment lumen while 4 control animals (DMSO-treated, n = 9) had lumen. This observation supports the idea that iCRT14 treatment delays intestine regeneration. In contrast, the gut rudiment area in animals treated with LiCl was significantly larger (about 100%) compared to the control group (NaCl-treated) (Fig. 2H). These findings suggest that the canonical Wnt signaling pathway might be involved in intestine regeneration of *H. glaberrima* and that its presumed activation is associated with the formation of the regenerating intestinal rudiment.

**A. Effects of putative Wnt signaling pathway modulators on cell dedifferentiation, proliferation and apoptosis-—**We then set to determine whether the drugs had an effect on the cellular events known to play important roles in the intestinal regeneration process: cellular dedifferentiation, cellular proliferation, and apoptosis.

**Cellular dedifferentiation-:** Following evisceration, cells within the remaining mesentery undergo a process of dedifferentiation. This process is particularly noticeable in the mesentery muscle layer, where muscle fibers disappear and form spindle-like structures (SLSs) that contain the remnants of the contractile machinery. SLSs are easily detected using fluorescent-labeled phalloidin (García-Arrarás et al., 2011). The formation of SLSs, and thus muscle dedifferentiation, occurs in a gradient, beginning at the tip of the mesentery, where autotomy has occurred, and increases with time, moving toward the body wall (Fig. 3A). At 7–10 dpe, SLSs are typically observed in the proximal (adjacent to the body wall) (Fig. 3B) and the middle (Fig. 3C) segments of the mesentery. At this regenerative stage both SLSs and muscle fibers have disappeared from the distal segment (adjacent to the gut rudiment) (Fig. 3D) and from the gut rudiment (Fig. 3E) while the proximal section of the mesentery still has most of its muscle fibers intact (Figs. 3B). Thus, a basic analysis of the degree of muscle dedifferentiation was performed by determining the localization of SLSs in the mesentery relative to the gut rudiment and the body wall as indicated in Fig. 4A. This analysis provides an overview of the regeneration process and in particular serves to determine, in a semi-quantitative way, if the formation and development of the dedifferentiation gradient is altered by the experimental treatment (Pasten et al., 2012). SLSs in iCRT14-treated animals were mainly observed within the distal segment of the mesentery (Figs. 4B–C) whereas in control animals (DMSO-treated) SLS were mainly observed within the middle segment of the mesentery (Figs. 4D–E). Furthermore, SLSs were observed within the middle segment of the mesentery in both LiCl (Figs. 4G–H) and NaCl treated groups (Figs. 4I–J). We found that the average score assigned to iCRT14-treated animals (2.4) was significantly lesser than the score of the control group (4.1) (Fig. 4F). However, we did not observe significant differences in SLSs scores between LiCl-treated (3.6) and control group (3.8) animals (Fig. 4K). These results suggest that the putative Wnt pathway inhibition *in vivo* lead to a delay in muscle dedifferentiation whereas the alleged Wnt pathway activation *in vivo* has no apparent effects on the muscle dedifferentiation gradient during intestine regeneration.

**Cell proliferation-:** An increase in cell proliferation in the intestinal rudiment and adjacent mesentery of regenerating animals has also been documented to take place during intestinal regeneration (García-Arrarás et al., 2011). The prevailing hypothesis is that, during the regenerative event, dedifferentiated cells re-enter the cell cycle and constitute an important source of cells for the gut rudiment growth (García-Arrarás et al., 1998, 2011). Thus, we evaluated the effects of alleged Wnt pathway modulators on cell proliferation in the regenerating intestines. After 9–10 days of treatment, we observed BrdU labeled nuclei in the mesothelium of gut rudiments of both iCRT14 (Fig. 5A) and LiCl (Fig. 5D) treated animals and their controls (Figs. 5B & 5E, respectively). We found that iCRT14 led to a significant reduction (about 30%) in the percentage of BrdU labeled nuclei in the gut rudiment mesothelium of treated animals when compared to controls (DMSO-treated) animals (Fig. 5C). However, we did not observe significant differences in the proliferation rate between LiCl treated animals and their controls (NaCl-treated) (Fig. 5F). These results suggest that the putative Wnt pathway inhibition affects cell proliferation during intestinal regeneration *in vivo*.

**Apoptosis-:** A transient increase in programmed cell death in the mesothelium of the gut rudiment and adjacent mesentery of regenerating intestines has also been documented (Mashanov et al., 2010). Here we evaluated the effects of presumed canonical Wnt pathway modulators on regenerating intestines by measuring apoptosis. We observed TUNEL labeled cells in the mesothelium of gut rudiments of both iCRT14 (Figs. 6A & 6C) and LiCl (Figs. 6F & 6H) and their controls (Figs. 6B & 6D & Figs. 6G & 6I, respectively). However, we did not find significant differences in the percentage of apoptotic cells between iCRT14 or LiCl treated animals and their respective controls after 10–11 days of treatment (Figs. 6E & 6J, respectively). These results do not support an effect of the putative Wnt pathway modulators on programmed cell death during intestinal regeneration in *in vivo* experiments.

The outcome of the *in vivo* experiments shows a striking effect of drugs that have been shown to modulate the Wnt pathway in other species, on the size of the regenerating rudiment and some effects on cell division and proliferation of *H. glaberrima*. However, *in vivo* studies are notoriously complicated by high variability, possible drug side-effects and by the difficulty of maintaining a constant drug concentration in aquatic animals. Therefore, for an in depth analysis on a possible role of Wnt signaling in the regenerative process and at the same time narrow down the cellular events that might be affected, we decided to move to our recently developed *in vitro* explant system (Bello et al., 2015).

## 2. In Vitro studies

Initial *in vitro* experiments were done using, once again, iCRT14 and LiCl as putative Wnt pathway modulators.

### A. iCRT14 and LiCl induce changes in regeneration-associated cellular events in tissue explants.—

Intestine explants dissected from sea cucumbers that had been eviscerated 4 days before were exposed to either iCRT14 for 72h or LiCl for 48–72h. Control explants were treated with 0.2% DMSO or 20mM NaCl, respectively. Histological

sections of the explants were evaluated for cellular dedifferentiation, cellular proliferation and apoptosis.

**Cellular dedifferentiation-:** We evaluated the effects of the putative modulators on muscle dedifferentiation *in vitro* using a more quantitative analysis from the one performed *in vivo*. While we determined the gradient of muscle dedifferentiation *in vivo* (the relative localization of SLSs in the mesentery with respect to the gut rudiment), *in vitro* we quantified the ratio of SLSs/nuclei between treated explants and their respective controls. For each explant we counted both the number of SLSs and cell nuclei in three different regions of the mesentery to obtain the SLSs/nuclei ratio per explant. SLSs were observed in both iCRT14 (Figs. 7A & 7C) and LiCl (Figs. 7F & 7H) treated explants and their controls (Figs. 7B & 7D & Figs. 7G & 7I). We found a significant reduction in the SLS/DAPI ratio (about 42%) in iCRT14-treated explants compared to the vehicle group (DMSO-treated) (Fig. 7E). iCRT14-treated explants also presented a higher number of muscle fibers (less muscle dedifferentiation) in the proximal end of the mesentery (Fig. 7C), compared to the vehicle group (Fig. 7D). Explants treated with LiCl exhibited a disorganized amorphous tissue structure with no distinguishable properties of a rudiment or mesenteries (Fig. 7F) while a defined gut rudiment and mesentery were observed in control group explants (Fig. 7G). SLSs were observed scattered in the explants treated with LiCl (Fig. 7F & 7H). Additionally, we found that the SLS/DAPI ratio was significantly greater (about 169%) in LiCl-treated explants compared to control (NaCl-treated) explants (Fig. 7J). LiCl-treated explants were more fragile compared to controls and we had to be careful during their manipulation to obtain tissue sections without ruptures. These results suggest that, *in vitro*, putative inhibition of the canonical Wnt pathway using iCRT14 reduces muscle dedifferentiation while LiCl increases muscle dedifferentiation.

**Cell proliferation-:** We also tested the effect of alleged Wnt pathway modulators on cell proliferation *in vitro*. We observed BrdU-labeled cell nuclei in both iCRT14 (Figs. 8A) and LiCl-treated (Fig. 8D) explants and their respective controls (Figs. 8B & 8E). When the percentage of BrdU-labeled cells was quantified, we found that iCRT14 treatment led to a significant reduction (about 50%) compared to control group (Fig. 8C). However, we also found that the percentage of BrdU-labeled cells was significantly smaller (about 70%) in LiCl-treated explants compared to controls (NaCl-treated) (Fig. 8F). These results suggest that both iCRT14 and LiCl reduce the proliferation rate in regenerating gut explants.

**Apoptosis-:** To determine if the putative modulators of the Wnt canonical pathway have an effect on apoptotic cell death we used the TUNEL assay to measure apoptosis following treatment of gut explants with iCRT14 or LiCl for 72h. We observed TUNEL labeled cells in the mesothelium of both iCRT14 (Figs. 9A & 9C) and LiCl (Figs. 9F & 9H) treated explants and their controls (Figs. 9B & 9D & Figs. 9G & 9I, respectively). However, we did not find significant differences in the percentage of apoptotic cells between iCRT14 or LiCl treated explants and their respective controls (Figs. 9E & 9J, respectively). These results do not support an effect of the presumed Wnt pathway modulators on programmed cell death during intestinal regeneration *in vitro*.

**B. Differential effects on cell proliferation and cell dedifferentiation of LiCl doses—**The experimental results with LiCl were surprising in that, similar to iCRT14, it caused a decrease in cell proliferation. Our next step was to determine if these effects were due to the drug dose. To evaluate the effect of LiCl, we took advantage of the fact that at 14 dpe, gut rudiments already have luminal epithelium. Therefore, by using 14 dpe explants we could evaluate the LiCl effect on cell proliferation both in mesothelium and in the luminal epithelium. In this way we could test if the LiCl effect was dose dependent and at the same time if the cell proliferation inhibition was limited to mesothelial cells. We exposed gut explants from 14 dpe animals to 2, 10, or 20 mM LiCl for 48h. Histological sections of the explants were evaluated for cell proliferation and cell dedifferentiation.

**Cell proliferation-:** We observed BrdU-labeled cells in both the mesothelium (Fig. 10 A,D,G) and luminal epithelium (Fig. S1 A,D,G) of explants treated with all LiCl doses and in controls (Fig. 10 B,E,H & Fig. S1 B,E,H, respectively). The proliferation rate in both mesothelium and luminal epithelium of explants treated with 20 mM was significantly smaller compared to controls (Fig. 10I & Fig. S1I, respectively). In contrast, cell proliferation was not affected in the mesothelium (Fig. 10F & 10C) or luminal epithelium (Figs. S1F & S1C) of explants treated with either 10 or 2 mM LiCl compared to their respective controls. Overall, our results suggest that the higher dose (20mM) of LiCl reduces cell proliferation in both mesothelial and luminal epithelial cells in gut explants.

**Cellular dedifferentiation-:** We evaluated qualitatively the ability of LiCl to promote muscle dedifferentiation determining the disappearance of the gut rudiment muscle layer and the concomitant appearance of SLSs. We found that explants treated with 20 mM LiCl exhibited SLSs and spherical to irregular cells labeled with phalloidin in lieu of a defined muscle layer (Fig. 11J, yellow arrows). Conversely, control explants showed a defined muscle layer in the gut rudiment mesothelium (Fig. 11L, white arrows). We found that 3 of the 5 explants (n = 5) treated with 10 mM LiCl exhibited a defined muscle layer in the gut rudiment (Fig. 11F) similar to that observed in control explants (Fig. 11H) and both groups exhibited similar explant morphology (Figs. 11E & 11G). However, the remaining two explants exhibited SLSs instead of a defined muscle at the gut rudiment. They also showed altered explant morphology similar to explants treated with 20 mM LiCl (not shown). Finally, all explants treated with 2mM LiCl showed a defined muscle layer in the gut rudiment mesothelium (Fig. 11B) similar to that observed in control explants (Fig. 11D) and they also exhibited similar morphology (Figs. 11A & 11C). Overall, our results suggest that LiCl promotes gut rudiment muscle dedifferentiation in doses of 20 and 10 mM but not at 2mM.

**C. Use of additional putative Wnt signaling pathway modulators to evaluate cell dedifferentiation and cell proliferation—**Many signaling pathways share overlapping components among them. In particular, Wnt signaling can cross-talk with other signaling pathways providing added complexity to the unraveling of signaling mediators. Thus, to investigate whether the effects we observed rely primarily on Wnt signaling we employed additional drugs that have been shown to modulate the Wnt signaling pathway in other species to determine their effects in our system. In addition, several doses of some

drugs were tested in order to determine possible dose-related effects. Table 1 summarizes the effects of the already described (iCRT14 and LiCl) and of additional small molecules tested as putative Wnt pathway modulators on cell proliferation and muscle dedifferentiation in gut explants after 72h of treatment.

We tested two additional putative Wnt pathway activators, 1-Azakenpaullone (Kunick et al., 2004) and CHIR99021 (Eldar-Finkelman and Martinez, 2011) and one additional inhibitor, Wnt-C59 or C59 (Proffitt et al., 2013) in explants. Both 1-Azakenpaullone and CHIR99021 activate the canonical Wnt pathway by inhibiting the enzyme GSK-3 in the same manner as LiCl does; however, they are more specific for GSK-3 than LiCl (Kunick et al., 2004; Eldar-Finkelman and Martinez, 2011). We evaluated three doses of 1-Azakenpaullone (100, 20, and 2 μM) and two doses of CHIR99021 (20 and 5 μM) and found that 1-Azakenpaullone (at doses of 100–20 μM) and CHIR99021 (at a dose of 20 μM) showed similar effects to those caused by 20 mM LiCl on muscle dedifferentiation and cell proliferation. Specifically, both increased the SLS/DAPI ratio (about 50% and 30%, respectively) compared to controls (Figs. 12 A–E & 12 F–J, respectively) whereas they led to a significant reduction in cell proliferation rate (about 60% in both cases) compared to control explants (DMSO-treated) (Figs. 13 A–C and 13 D–F, respectively). The 1-Azakenpaullone and CHIR99021 treated explants (at the doses mentioned above) were also more fragile compared to controls. We had to be careful during their manipulation to obtain tissue sections without ruptures. Finally, the lower doses tested, 2 μM for 1-Azakenpaullone and 5 μM for CHIR99021, did not affect muscle dedifferentiation or cell proliferation.

C59 (Proffitt et al., 2013), which is known to inhibit the enzymes required for the processing and secretion of Wnt molecules, was tested at three different doses (15, 5, 1 μM). None of the doses affected the muscle dedifferentiation compared to controls (DMSO) (Figs. 12 K–O); however, the highest dose tested of C59 (15 μM) caused a significant reduction (about 43%) in the percentage of BrdU positive cells compared to controls (DMSO) (Fig. 13 G–I).

Other putative Wnt pathway modulators were tested, but none of these showed effects on cell dedifferentiation or cell division in explants (See Table S1). These include the Wnt activator SKL2001 (a.k.a. Wnt agonist II) (Gwak et al., 2012) at doses of 200, 50, and 5 μM, and the inhibitors EGCG (Kim et al., 2006) at doses of 500, 150 and 50 μM, and XAV939 (Huang et al., 2009), at doses of 100, 50, and 15 μM. Since most of these drugs have been developed for vertebrate systems (and mainly mammals), it is impossible to conclude that their lack of effect in our system reflects the non-involvement of the Wnt signaling pathway. The possibility that they are species specific and simply not effective in echinoderm tissues at the doses used remains an alternate explanation for their lack of action.

In summary, our results show that several putative modulators of the Wnt signaling pathway have an effect on the cell dedifferentiation and proliferation but not on the apoptosis that accompanies intestinal regeneration (See Table 1). Nonetheless, when the specific actions of each drug are analyzed, a pattern emerges that suggests that only those that inhibit the enzyme GSK-3 increase the muscle dedifferentiation, while the small molecules that act at other levels did not affect (most of them) or reduce (in the case of iCRT14) the muscle dedifferentiation.

**D. PY489-β-catenin is overexpressed in the gut rudiment at 7 dpe *in vivo*—**An alternative way of determining the involvement of the Wnt pathway in intestinal regeneration is to probe the activation state of β-catenin. This can be done by localizing β-catenin within the cell nuclei and by determining the phosphorylated state of the molecule. For this, we used an antibody that recognizes β-catenin when phosphorylated on Tyr 489 (PY489-β-catenin). Previous studies have demonstrated that PY489-β-catenin is targeted to the nucleus (referred to as nuclear β-catenin), corresponding to a transcriptionally activated form of β-catenin (Rhee et al., 2007; Zhu et al., 2014). This antibody was then used to determine the percent of positive β-catenin cells in the holothurian tissues.

We found that in intestinal tissues of normal, non-eviscerated animals, PY489-β-catenin antibody specifically labels scattered cell nuclei located mainly in the luminal epithelium (not shown) and in the outer layer of the mesothelium (Figure 14A) as well as in the normal mesenterial mesothelium (Fig. 14B). In animals that had been eviscerated and were undergoing regeneration PY489-β-catenin labeling was expressed in the regenerating rudiment at all stages of regeneration from 3 dpe up to 14 dpe (Fig. 14 C–D). At 3 dpe a small enlargement of the distal mesentery was observed while at 7 and 14 dpe a gut rudiment had already formed. We did not find a significant difference in the percentage of cells labeled in the 3-dpe mesentery mesothelium compared to that observed in normal intestine or normal mesentery (Fig. 14E). However, a significant increase in nuclear β-catenin labeling was observed in gut rudiments at 7 dpe compared to normal intestine, normal mesentery or to the mesenteric region of the 7 dpe regenerate (Figure 14 E–F). At 14 dpe the percentage of cell nuclei immunoreactive to the PY489-β-catenin antibody in gut rudiments decreases, returning to levels similar to those found in normal intestine or normal mesentery (Figure 14E). Thus, our results suggest that β-catenin is activated in the mesothelial cells of the regenerating rudiment primarily at 7 dpe (Fig. 14F).

**E. Wnt signaling inhibitor C59 reduces the expression level of PY489-β-catenin *in vitro*—**We now wanted to determine the effect that pharmacological agents used in other model systems as modulators of the Wnt pathway (both agonists and antagonists) might have on the expression of PY-489-β-catenin in gut explants as an indicator of Wnt signaling disruption. For this we treated gut explants dissected at 4 dpe for 72h with putative Wnt pathway modulators (See Table 1 and Table S1, respectively). We tested only the highest dose of each of the modulators. The presumed Wnt agonists evaluated were 20 mM LiCl, 100 μM 1-Azakenpaullone, 20 μM CHIR99021, and 200 μM SKL2001. The alleged Wnt antagonists tested were 50 μM iCRT14, 15 μM C59, and 100 μM XAV-939. Surprisingly, none of the putative Wnt activators showed an effect on the PY489 labeling (Figs. S2 & S3). Among the presumed Wnt antagonists, only C59 at a dose of 15 μM (the same dose that decreases cell proliferation) decreased the number of cells expressing nuclear β-catenin in gut explants (Figures 14 G–I). This implies that the putative activators and some of the alleged inhibitors of the canonical Wnt pathway did not affect the expression levels of the transcriptionally activated form of β-catenin in holothurian gut explants. However, decreasing the levels of secreted Wnts via C59 treatment does show an effect on the activated (phosphorylated) β-catenin molecule.

## Discussion

### Wnt and regeneration-

The *in vivo* and *in vitro* results shown here strongly suggest that Wnt-signaling plays a role in the regulation of cellular events during early intestinal regeneration. Previous work from our laboratory and that of others has provided evidence for the involvement of Wnt in intestinal regeneration of sea cucumbers, specifically the finding that Wnt-ligand and frizzled receptor homologs in sea cucumbers (*H. glaberrima, A. japonicus, and E. fraudratrix)* are up-regulated during intestinal regeneration and that transcripts for Wnt-9 are mainly found within the regenerating rudiment and the adjacent mesentery (Ortiz-Pineda et al., 2009; Mashanov et al., 2012; Sun et al., 2013; Girich et al., 2017; Yuan et al., 2019). We now extend these results by showing that *in vivo* intestinal regeneration is altered by putative modulators of the Wnt signaling pathway; LiCl enhances the formation of the intestinal rudiment (increasing the rudiment size) while iCRT14 causes a reduction in the size of the rudiment. These two drugs have been shown to act as Wnt signaling modulators in various species. LiCl activation of the Wnt signaling is widely supported by *in vivo* and *in vitro* experimental evidence (Klein and Melton, 1996; Stambolic et al., 1996; Jope, 2003) and in particular it has been used regularly to study developmental processes in echinoderms (Logan et al., 1999). On the other hand, iCRT14 is an antagonist that disrupts the activation of Wnt-target genes (Gonsalves et al., 2011) and has been shown to block developmental and regenerative processes in coelenterates (Gufler et al., 2018).

Our results agree with those of other investigators that have shown Wnt involvement in regenerative events in animals with strong regenerative abilities. For example, Wnt pathway is required for *Hydra* head regeneration (Broun et al., 2005; Chera et al., 2009) and for the correct anterior-posterior patterning during planarian and acoels regeneration (Gurley et al., 2008; Tanaka and Weidinger, 2008; Srivastava et al., 2014). This signaling pathway is also required for the proper regeneration of fins, retina, and spinal cord in zebrafish (Wehner et al., 2014; Ramachandran et al., 2011; Strand et al., 2016) and limbs in *Xenopus* tadpoles (Yokoyama et al., 2007). Additionally, the Wnt/β-catenin pathway is required during skeletal muscle regeneration in mammals (Rudolf et al., 2016). In particular our results can be compared to those observed by Stoick-Cooper et al. (2007), where Wnt pathway activation during fin regeneration in zebrafish resulted in increased length of fins, and conversely, Wnt signaling inhibition led to impairment of fin regeneration. Similar effects of Wnt signaling modulation were observed in injured retinas of rodents and zebrafish (Osakada et al., 2007; Ramachandran et al., 2011). Thus, it is not surprising that Wnt signaling is associated to sea cucumber intestinal regeneration, in view of the large amount of data associating Wnt signaling and regeneration in many different tissues and animal models.

### What is the cellular mechanism of Wnt-signaling pathway modulation?

In order to be able to answer this question we need to recapitulate the cellular events that take place during intestine regeneration in *H. glaberrima*. This process takes place via a combination of epimorphic and morphallactic mechanisms (Mashanov and García-Arrarás, 2011). Both the reorganization of the remaining mesentery by cell dedifferentiation and migration and the formation of a blastema-like structure containing proliferating cells are

involved in gut regeneration. Our working model states that following evisceration, mesothelial cells at the injury site dedifferentiate and migrate toward the tip of the mesentery where they proliferate and form the epithelium of the regenerating blastema-like structure (or rudiment) (García-Arrarás et al., 2018a 2018b). Eventually some of these cells undergo epithelial to mesenchymal transition and enter the underlying connective tissue (Mashanov and García-Arrarás, 2011; García-Arrarás et al., 2011). Therefore, the mechanisms by which putative Wnt modulators increase the size of the rudiment could involve an increase in cell dedifferentiation, a reduction in cell death, an increase in cell proliferation, or a combination of these. Our data suggest that we can discard a role for apoptosis in this phenomenon since we did not find an effect of Wnt pathway modulators on apoptosis. Thus, even though apoptosis is transiently increased in gut rudiment during intestine regeneration (Mashanov et al., 2010), and even though there is some experimental data on a role of apoptosis on regenerative processes (Bodine, 2008), our results agree with other studies that showed an effect of Wnt pathway activation on cell differentiation and cell proliferation but not on apoptosis (Famili et al., 2016).

Of the two remaining cellular events that were studied, one would expect a combination of increased cell dedifferentiation and proliferation by the alleged Wnt-pathway activator and a decrease of the same cell mechanisms by the putative inhibitor to explain the observed changes in rudiment size. The expected results agree with the effects of the inhibitor iCRT14. However, in *in vivo* experiments, LiCl did not activate cellular dedifferentiation or cell proliferation.

It is difficult to explain these results, however we need to take into account that first, LiCl is known to have multiple effects that are independent of the Wnt-signaling pathway (Pardo et al., 2003) and therefore some of these side effects might be interfering with the regeneration process. Second, we are collecting data a week after regeneration has begun, thus we might be missing some possible early effects. Finally, there is an additional process that is known to be modulated by the Wnt/β-catenin pathway that we did not study: cell migration (Neth et al., 2006). It is important to highlight that during intestinal regeneration in *H. glaberrima*, the dedifferentiated cells are thought to migrate toward the free end of the mesentery where they form the blastema-like structure. Thus, it is utterly possible that putative Wnt pathway modulators are having an effect in the migration of these cells that causes major changes in the size of the regenerating rudiment.

In summary, our *in vivo* results point toward cell dedifferentiation and cell proliferation, but not apoptosis, as possibly being involved in the observed changes in rudiment size after treatment with alleged Wnt/βcatenin signaling pathway modulators. A more in depth analysis of these possibilities was probed in our *in vitro* experiments.

### Wnt pathway regulation of cell proliferation

Canonical Wnt pathway inhibition using various chemical agents have been shown to decrease cell proliferation *in vitro* (Ono et al., 2014). Therefore, it was no surprise to observe that iCRT14 led to a significant reduction in cell proliferation both *in vitro* and *in vivo*. These results agree with those obtained by Gonsalves et al. (2011) who found that the proliferation rate of grafted cancer cells was reduced in iCRT14-treated animals. The finding

that not all putative Wnt inhibitors tested caused a decrease in cell proliferation was somewhat perplexing. However, let us not forget that most of these drugs have been developed for their action on mammalian tissues and little or nothing is known of their interactions or effects on invertebrate cells and in particular on those of echinoderms. Therefore, we need to focus on those drugs that did show an effect, and in this case two putative Wnt signaling pathway inhibitors (iCRT14 and C59) with different inhibitory mechanisms were shown to reduce cell proliferation. iCRT14 disrupts the interaction between β-catenin and the TCF/LEF complex, a step that is found at the end of the Wnt-signaling pathway (Gonsalves et al., 2011). C59, on the other hand, acts at the beginning of the signaling path by inhibiting the enzyme porcupine that mediates the O-palmitoylation of all Wnt ligands, which is a modification required for Wnt ligand secretion (Proffitt et al., 2013). Therefore, our data suggests that inhibiting the Wnt signaling pathway, either at its inception or at the end of the pathway has a negative effect on cell proliferation.

In contrast, inhibition of cell proliferation by some presumed Wnt pathway activators (LiCl, 1-Azakenpaullone, CHIR99021) was somewhat unexpected. LiCl (as well as other activators) is classically known to promote activation of cell proliferation via an inhibition of the enzyme GSK-3, which then results in an increase in nuclear β-catenin levels. However, although an increase in cell proliferation has been well documented, such as in human mesenchymal stem cells (Neth et al., 2006), zebrafish retinal progenitor cells (Ramachandran et al., 2011) and mouse Sertoli cells (Li et al., 2012), LiCl has also been documented, as well, to inhibit cell proliferation. This has been shown mainly in cancer cells such as embryonal carcinoma cells and human neuroepithelioma cells (Smits et al., 1999), human osteosarcoma and colon carcinoma cells (Kaufmann et al., 2011), but also in primary cell cultures of vascular smooth muscle (Wang et al., 2013), bovine aortic endothelium (Mao et al., 2001), and rat intervertebral discs (Hiyama et al., 2011).

Among the mechanisms that have been proposed to explain LiCl decrease in proliferation in other systems are: 1) an inhibition of cytosolic enzymes other than GSK-3, such as inositol monophosphatase (IMPase) (Phiel and Klein, 2001; Cohen and Goedert, 2004); 2) an inhibition of other signaling pathways (Pardo et al., 2003); 3) a reduction in molecules directly involved in cell cycle regulation (Wang et al., 2013); 4) a stabilization of the tumor suppressor protein p53 and its accumulation in the cytoplasm (Mao et al., 2001). In this respect it is important to highlight that the three alleged Wnt signaling activators that showed an inhibition of cell proliferation in sea cucumbers, LiCl, 1-Azakenpaullone, and CHIR99021, act by inhibiting GSK-3 (Klein and Melton, 1996; Kunick et al., 2004; Eldar-Finkelman and Martinez, 2011, respectively). Thus, we propose that the mechanism by which cell proliferation is being inhibited in the intestinal regeneration model is by the inhibition of a GSK-3 that participates in a signaling pathway other than the Wnt signaling pathway (see a lengthier discussion of this topic in the section below).

Additional support for a role of the canonical Wnt signaling pathway in the cell proliferation taking place during early intestinal regeneration comes from our immunohistological studies. First, temporal and spatial changes in the phosphorylation of β-catenin detected by the PY-489-β-catenin antibody correlate with previous cell division findings; the increase observed in PY-489-β-catenin labeling mainly occurs in the mesothelium of the 7-dpe

intestinal rudiment, the same location and timing that has been shown for the peak of cell proliferation (García-Arrarás et al., 1998; 2011; 2018). Second, C59, a Wnt pathway inhibitor that causes a decrease in cell proliferation in the regenerating explants, also causes a similar decrease in the labeling of PY-489 labeled cells.

In summary, it is safe to state that most of our data point to an involvement of Wnt signaling pathway in the cell proliferation that takes place during early regeneration of the intestinal organ of holothurians. These data include the effect of drugs at different levels of the signaling pathway as well as the spatial and temporal changes observed in β-catenin expression in control and experimental animals.

### A Wnt-independent GSK-3 mediated signaling pathway activates muscle dedifferentiation

In contrast to a possible role of Wnt signaling on cell proliferation, our data suggest no such role on the process of cell dedifferentiation. Although we initially found that LiCl promoted, whereas iCRT14 blocked muscle dedifferentiation in gut explants, the effect of other drugs and in particular their mode of action need to be analyzed to reach an appropriate conclusion.

The fact that C59, which in the same system inhibits cell proliferation, has no effect on muscle dedifferentiation provides a strong argument against Wnt-signaling mediation of cell dedifferentiation during intestinal regeneration. Nonetheless, we still need to explain why the putative antagonist iCRT14 showed an effect on muscle dedifferentiation. A possible explanation is that this antagonist interferes with the association of β-catenin with transcription factors (Tcf) and therefore with the gene expression action of the signaling pathway (Yan et al., 2017). Thus, it is possible that this site of action is shared or interferes with those of other signaling pathways and also causes the inhibition of the dedifferentiation process.

Immunohistochemical experiments detecting the localization of phosphorylated β-catenin provide additional evidence against the involvement of the Wnt/β-Catenin pathway in the cellular dedifferentiation process. First, there is no spatial or temporal correlation between the muscle dedifferentiation and the increase in PY-489-β-catenin labeling *in vivo*; dedifferentiation takes place throughout the mesentery while the increase in PY-489-β-catenin labeling is mainly observed in the gut rudiment at 7 dpe (See Figure 14F). Similarly, dedifferentiation is already occurring at 3dpe, while an increase in PY-489-β-catenin labeling is not observed at that stage *in vivo*. In addition, pharmacological treatments that cause an increase or decrease in dedifferentiation *in vitro*, had no effect on PY-489-β-catenin labeling.

The three putative Wnt agonists tested (LiCl, 1-Azakenpaullone, and CHIR99021) provide clues to decipher the signaling mechanism of muscle dedifferentiation. While the use of LiCl has already been discussed, the other two molecules, 1-Azakenpaullone and CHIR99021, are considered more potent (used in the nanomolar range) and specific Wnt pathway activators than LiCl. 1-Azakenpaullone has been used to activate the Wnt pathway in models of regeneration such as zebrafish (Meyers et al., 2012). Conversely, CHIR99021 has been used mainly as Wnt pathway activator in mammal stem cells (Naujok et al., 2014). The three of

them act by inhibition of the enzyme GSK-3 (Klein and Melton, 1996, Kunick et al., 2004, Eldar-Finkelman and Martinez, 2011). Therefore most of the observed *in vitro* effects of the drugs on muscle dedifferentiation can be explained by their inhibition of GSK-3 or on the downstream signaling pathway.

In view of the observed drug effects we propose that GSK-3 is the mediator of the cellular dedifferentiation response, and that it takes place by a signaling pathway that is independent of Wnt. This is not surprising since it is well known that GSK-3 can have Wnt-independent effects by its activation or inactivation via different pathways. For example, it has been shown that vascular smooth muscle can be dedifferentiated via a GSK-3 inactivation mechanism (Frismantiene et al., 2016) and that this pathway is activated by Akt and not by Wnt. This is particularly interesting since echinoderm muscle is thought to be more akin to vertebrate smooth muscle than to skeletal muscle.

GSK-3 has also been associated with differentiation/dedifferentiation processes in other model systems. In chondrocyte dedifferentiation, researchers have documented an increase in the active form of β-catenin and the inactivation of GSK-3α/β forms (Charlier et al., 2016; Zhou et al., 2016). Similarly, in cardiac muscle, GSK-3 inhibition increased β-catenin accumulation and cellular dedifferentiation as determined by the expression of dedifferentiation markers (D'Uva et al., 2015). Finally, in zebrafish GSK-3 inhibition was sufficient to stimulate Müller glia dedifferentiation into proliferating progenitors (Ramachandran et al., 2011).

## Uncoupling of cellular processes

One of the interesting findings that emerge from our experimental results is the uncoupling of cellular events that take part in the initial regeneration process. While cell dedifferentiation, proliferation and apoptosis occur almost concomitantly soon after evisceration, different drug treatments are found to activate certain ones without affecting the others. Thus, we observe that drugs that cause an increase or decrease in dedifferentiation or cell proliferation have no effect on apoptosis. More surprising is the uncoupling of the dedifferentiation response from cell proliferation as is observed with C59 or with the GSK3 inhibitors where cell proliferation decreases while cell dedifferentiation either does not change or increases. Particularly, since canonical Wnt signaling has been associated with modulation of both cell dedifferentiation and cell cycle re-entry (Teo and Kahn, 2010). Nonetheless, there is experimental evidence that they can be modulated independently one from the other. For example, during limb regeneration in salamanders, muscle fibers can undergo the process of dedifferentiation even after cell proliferation arrest by X-irradiation, or upregulation of p16 (Velloso et al., 2000). Similarly, Schwann cells derived from adult rats are able to dedifferentiate *in vitro* without entering the cell cycle when stimulated with cAMP. Proliferation is triggered by mitogens such as neuregulins in these cells (Monje et al., 2010). Even in plants it has been shown that when the cell wall is removed from mesophyll cells (non-dividing plant cells), they become stem-like cells (pluripotential cells) *in vitro*, however, these dedifferentiated cells can re-enter the cell cycle or not depending on the molecules present in the cell culture medium (Zhao et al., 2001).

Our findings identify GSK-3 as the key common intersection of the cell proliferation and cell dedifferentiation processes, where when inhibited, cell proliferation decreases while cell dedifferentiation increases. Our working model would be that GSK-3 participates in a hitherto undetermined pathway and that when inhibited, causes muscle dedifferentiation and inhibits cell proliferation. Thus, the effect of GSK-3 in this proposed pathway supersedes the GSK-3 inhibition of the Wnt signaling pathway that would normally result in increased cell division. In this scenario, it is interesting to compare our results with those showing that GSK-3 is involved in cardiomyocyte dedifferentiation during regeneration (D'Uva et al., 2015). In this model they also observed a decoupling between muscle dedifferentiation, cell proliferation and hypertrophy and showed that they could be uncoupled by ERK, AKT and GSK-3/β-catenin signaling.

In conclusion, our results provide novel insights into the signaling systems that mediate regenerative responses, and in particular those of intestinal regeneration. The findings that cell mechanisms associated with intestinal regeneration can be modulated independently together with the finding that cellular dedifferentiation appears to be controlled by GSK-3 signaling, open a door for future studies. At the same time, new questions arise; which signaling pathways cause the proposed GSK-3 inhibition? What signaling pathways and cellular events are responsible for the LiCl induced increase in rudiment size *in vivo*? The answer to these and other questions will be the focus of future experiments to characterize the signaling pathways that are involved in the process of intestinal regeneration in the sea cucumber and that might be common to regenerative processes in other animals.

## Supplementary Material

Refer to Web version on PubMed Central for supplementary material.

## Acknowledgments

This project was funded by NIH (Grant R15NS01686), NSF (IOS-0842870), RISE NIH (Grant 5R25GM061151), and the University of Puerto Rico. Many experiments were made possible by a PR Hurricane Relief Grant from the Society of Developmental Biology. We also acknowledge partial support to Samir A. Bello from the University of Puerto Rico through the Merit and Doctoral Dissertation Fellowships.

## References

Adell T, Marsal M, Saló E, 2008 Planarian GSK3s are involved in neural regeneration. Dev. Genes Evol 218, 89–103. doi:10.1007/s00427-007-0199-3 [PubMed: 18202849]

Bello SA, Abreu-Irizarry RJ, García-Arrarás JE, 2015 Primary cell cultures of regenerating holothurian tissues. Methods Mol. Biol 1189, 283–97. doi:10.1007/978-1-4939-1164-6_19 [PubMed: 25245701]

Bodine PVN, 2008 Wnt signaling control of bone cell apoptosis. Cell Res. 18, 248–253. doi: 10.1038/cr.2008.13 [PubMed: 18212734]

Broun M, Gee L, Reinhardt B, Bode HR, 2005 Formation of the head organizer in hydra involves the canonical Wnt pathway. Development 132, 2907–2916. doi:10.1242/dev.01848 [PubMed: 15930119]

Candelaria AG, Murray G, File SK, García-Arrarás JE, 2006 Contribution of mesenterial muscle dedifferentiation to intestine regeneration in the sea cucumber Holothuria glaberrima. Cell Tissue Res. 325, 55–65. doi:10.1007/s00441-006-0170-z [PubMed: 16541286]

Charlier E, Malaise O, Zeddou M, Neuville S, Cobraiville G, Deroyer C, Sanchez C, Gillet P, Kurth W, de Seny D, Relic B, Malaise MG, 2016 Restriction of spontaneous and prednisolone-induced leptin production to dedifferentiated state in human hip OA chondrocytes: Role of Smad1 and β-catenin activation. Osteoarthr. Cartil 24, 315–324. doi:10.1016/j.joca.2015.08.002 [PubMed: 26318657]

Chera S, Ghila L, Dobretz K, Wenger Y, Bauer C, Buzgariu W, Martinou JC, Galliot B, 2009 Apoptotic Cells Provide an Unexpected Source of Wnt3 Signaling to Drive Hydra Head Regeneration. Dev. Cell 17, 279–289. doi:10.1016/j.devcel.2009.07.014 [PubMed: 19686688]

Clevers H, Nusse R, 2012 Wnt/B-catenin signaling and disease. Cell 149, 1192–1205. doi:10.1016/j.cell.2012.05.012 [PubMed: 22682243]

Cohen P, Goedert M, 2004 GSK3 inhibitors: development and therapeutic potential. Nat. Rev. Drug Discov 3, 479–487. doi:10.1038/nrd1415 [PubMed: 15173837]

Cormier KW, Woodgett JR, 2017 Recent advances in understanding the cellular roles of GSK-3. F1000Research 6, 167. doi:10.12688/f1000research.10557.1

D'Uva G, Aharonov A, Lauriola M, Kain D, Yahalom-Ronen Y, Carvalho S, Weisinger K, Bassat E, Rajchman D, Yifa O, Lysenko M, Konfino T, Hegesh J, Brenner O, Neeman M, Yarden Y, Leor J, Sarig R, Harvey RP, Tzahor E, 2015 ERBB2 triggers mammalian heart regeneration by promoting cardiomyocyte dedifferentiation and proliferation. Nat. Cell Biol 17, 627–638. doi:10.1038/ncb3149 [PubMed: 25848746]

Devotta A, Hong C-S, Saint-Jeannet J-P, 2018 Dkk2 promotes neural crest specification by activating Wnt/β-catenin signaling in a GSK3β independent manner. Elife 7, 1–17. doi:10.7554/elife.34404

Dolmatov IY, Ginanova TT, 2001 Muscle Regeneration in Holothurians. Microsc. Res. Tech 55, 452–463. doi:10.1002/jemt.1190 [PubMed: 11782074]

Eldar-Finkelman H, Martinez A, 2011 GSK-3 Inhibitors: Preclinical and Clinical Focus on CNS. Front. Mol. Neurosci 4, 1–18. doi:10.3389/fnmol.2011.00032 [PubMed: 21441980]

Famili F, Brugman MH, Taskesen E, Naber BEA, Fodde R, Staal FJT, 2016 High Levels of Canonical Wnt Signaling Lead to Loss of Stemness and Increased Differentiation in Hematopoietic Stem Cells. Stem Cell Reports 6, 652–659. doi:10.1016/j.stemcr.2016.04.009 [PubMed: 27167156]

Frismantiene A, Dasen B, Pfaff D, Erne P, Resink TJ, Philippova M, 2016 T-cadherin promotes vascular smooth muscle cell dedifferentiation via a GSK3β-inactivation dependent mechanism. Cell. Signal 28, 516–530. doi:10.1016/j.cellsig.2016.02.014 [PubMed: 26907733]

García-Arrarás J, Estrada-Rodgers L, Santiago R, Torres II, Díaz-Miranda L, Torres-Avillán I, 1998 Cellular Mechanisms of Intestine Regeneration in the Sea Cucumber, Holothuria glaberrina Selenka (Holothuroidea: Echinodermata). J. Exp. Biol 281, 288–304.

García-Arrarás JE, Bello SA, Malavez S, 2018a The mesentery as the epicenter for intestinal regeneration. Semin. Cell Dev. Biol doi:10.1016/J.SEMCDB.2018.09.001

García-Arrarás JE, Dolmatov IY, 2010 Echinoderms: potential model systems for studies on muscle regeneration. Curr. Pharm. Des 16, 942–955. doi:10.2174/138161210790883426 [PubMed: 20041824]

García-Arrarás JE, Lázaro-Peña MI, Díaz-Balzac CA, 2018b Holothurians as a Model System to Study Regeneration, in: Results and Problems in Cell Differentiation. pp. 255–283. doi:10.1007/978-3-319-92486-1_13 [PubMed: 30083924]

García-Arrarás JE, Valentín-Tirado G, Flores JE, Rosa RJ, Rivera-Cruz A, San Miguel-Ruiz JE, Tossas K, 2011 Cell dedifferentiation and epithelial to mesenchymal transitions during intestinal regeneration in H. glaberrima. BMC Dev. Biol 11, 61. doi:10.1186/1471-213X-11-61 [PubMed: 22004330]

Girich AS, Isaeva MP, Dolmatov IY, 2017 Wnt and frizzled expression during regeneration of internal organs in the holothurian Eupentacta fraudatrix. Wound Repair Regen. 25, 828–835. doi:10.1111/wrr.12591 [PubMed: 28960616]

Gonsalves FC, Klein K, Carson BB, Katz S, Ekas L. a, Evans S, 2011 An RNAi-based chemical genetic screen identifies three small-molecule inhibitors of the Wnt / wingless signaling pathway. PNAS 108, 5954–5963. doi:10.1073/pnas.1017496108/-/DCSupplemental.www.pnas.org/cgi/doi/10.1073/pnas.1017496108 [PubMed: 21393571]

Gufler S, Artes B, Bielen H, Krainer I, Eder MK, Falschlunger J, Bollmann A, Ostermann T, Valovka T, Hartl M, Bister K, Technau U, Hobmayer B, 2018 β-Catenin acts in a position-independent

regeneration response in the simple eumetazoan Hydra. Dev. Biol 433, 310–323. doi:10.1016/j.ydbio.2017.09.005 [PubMed: 29108673]

Gurley KA, Rink JC, Sánchez-Alvarado A, 2008 B-Catenin Defines Head Versus Tail Identity During Planarian Regeneration and Homeostasis. Science (80-. ). 319, 323–327. doi:10.1126/science.1150029

Gwak J, Hwang SG, Park HS, Choi SR, Park SH, Kim H, Ha NC, Bae SJ, Han JK, Kim DE, Cho JW, Oh S, 2012 Small molecule-based disruption of the Axin/B-catenin protein complex regulates mesenchymal stem cell differentiation. Cell Res 22, 237–247. doi:10.1038/cr.2011.127 [PubMed: 21826110]

Hiyama A, Sakai D, Arai F, Nakajima D, Yokoyama K, Mochida J, 2011 Effects of a glycogen synthase kinase-3β inhibitor (LiCl) on c-myc protein in intervertebral disc cells. J. Cell. Biochem 112, 2974–2986. doi:10.1002/jcb.23217 [PubMed: 21678465]

Huang SMA, Mishina YM, Liu S, Cheung A, Stegmeier F, Michaud GA, Charlat O, Wiellette E, Zhang Y, Wiessner S, Hild M, Shi X, Wilson CJ, Mickanin C, Myer V, Fazal A, Tomlinson R, Serluca F, Shao W, Cheng H, Shultz M, Rau C, Schirle M, Schlegl J, Ghidelli S, Fawell S, Lu C, Curtis D, Kirschner MW, Lengauer C, Finan PM, Tallarico JA, Bouwmeester T, Porter JA, Bauer A, Cong F, 2009 Tankyrase inhibition stabilizes axin and antagonizes Wnt signalling. Nature 461, 614–620. doi:10.1038/nature08356 [PubMed: 19759537]

Hyman H, 1955 Echinodermata, in: The Invertebrates. McGraw-Hill, New York, Toronto, London, p. 763.

Jope RS, 2003 Lithium and GSK-3: One inhibitor, two inhibitory actions, multiple outcomes. Trends Pharmacol. Sci 24, 441–443. doi:10.1016/S0165-6147(03)00206-2 [PubMed: 12967765]

Jope RS, Johnson GVW, 2004 The glamour and gloom of glycogen synthase kinase-3. Trends Biochem. Sci 29, 95–102. doi:10.1016/j.tibs.2003.12.004 [PubMed: 15102436]

Kaufmann L, Marinescu G, Nazarenko I, Thiele W, Oberle C, Sleeman J, Blattner C, 2011 LiCl induces TNF-α and FasL production, thereby stimulating apoptosis in cancer cells. Cell Commun. Signal 9, 15. doi:10.1186/1478-811X-9-15 [PubMed: 21609428]

Kim J, Zhang X, Rieger-Christ KM, Summerhayes IC, Wazer DE, Paulson KE, Yee AS, 2006 Suppression of Wnt signaling by the green tea compound (−)-epigallocatechin 3-gallate (EGCG) in invasive breast cancer cells: Requirement of the transcriptional repressor HBP1. J. Biol. Chem 281, 10865–10875. doi:10.1074/jbc.M513378200 [PubMed: 16495219]

Klein PS, Melton D. a, 1996 A molecular mechanism for the effect of lithium on development. PNAS 93, 8455–8459. [PubMed: 8710892]

Komiya Y, Habas R, 2008 Wnt signal transduction pathways. Organogenesis 4, 68–75. doi:10.4161/org.4.2.5851 [PubMed: 19279717]

Kunick C, Lauenroth K, Leost M, Meijer L, Lemcke T, 2004 1-Azakenpaullone is a selective inhibitor of glycogen synthase kinase-3β. Bioorganic Med. Chem. Lett 14, 413–416. doi:10.1016/j.bmcl.2003.10.062

Li Y, Gao Q, Yin G, Ding X, Hao J, 2012 WNT/β-catenin-signaling pathway stimulates the proliferation of cultured adult human Sertoli cells via upregulation of C-myc expression. Reprod. Sci 19, 1232–40. doi:10.1177/1933719112447126 [PubMed: 22872488]

Logan CY, Miller JR, Ferkowicz MJ, McClay DR, 1999 Nuclear beta-catenin is required to specify vegetal cell fates in the sea urchin embryo. Development 126, 345–357. [PubMed: 9847248]

Mao CD, Hoang P, DiCorleto PE, 2001 Lithium inhibits cell cycle progression and induces stabilization of p53 in bovine aortic endothelial cells. J. Biol. Chem 276, 26180–8. doi:10.1074/jbc.M101188200 [PubMed: 11337498]

Mashanov VS, García-Arrarás JE, 2011 Gut regeneration in holothurians: A snapshot of recent developments. Biol. Bull 221, 93–109. [PubMed: 21876113]

Mashanov VS, Zueva OR, Garcia-Arraras JE, 2012 Expression of Wnt9, TCTP, and Bmp1/Tll in sea cucumber visceral regeneration. Gene Expr. Patterns 12, 24–35. doi:10.1016/j.gep.2011.10.003 [PubMed: 22079950]

Mashanov VS, Zueva OR, Rojas-Catagena C, Garcia-Arraras JE, 2010 Visceral regeneration in a sea cucumber involves extensive expression of survivin and mortalin homologs in the mesothelium. BMC Dev. Biol 10. doi:10.1186/1471-213X-10-117

Meyers JR, Hu L, Moses A, Kaboli K, Papandrea A, Raymond P. a, 2012 β-catenin/Wnt signaling controls progenitor fate in the developing and regenerating zebrafish retina. Neural Dev. 7, 30. doi: 10.1186/1749-8104-7-30 [PubMed: 22920725]

Monje PV, Soto J, Bacallao K, Wood PM, 2010 Schwann cell dedifferentiation is independent of mitogenic signaling and uncoupled to proliferation: Role of cAMP and JNK in the maintenance of the differentiated state. J. Biol. Chem 285, 31024–31036. doi:10.1074/jbc.M110.116970 [PubMed: 20634285]

Murray G, García-Arrarás JE, 2004 Myogenesis during holothurian intestinal regeneration. Cell Tissue Res. 318, 515–524. doi:10.1007/s00441-004-0978-3 [PubMed: 15480798]

Naujok O, Lentes J, Diekmann U, Davenport C, Lenzen S, 2014 Cytotoxicity and activation of the Wnt/beta-catenin pathway in mouse embryonic stem cells treated with four GSK3 inhibitors. BMC Res. Notes 7, 273. doi:10.1186/1756-0500-7-273

Neth P, Ciccarella M, Egea V, Hoelters J, Jochum M, Ries C, 2006 Wnt signaling regulates the invasion capacity of human mesenchymal stem cells. Stem Cells 24, 1892–1903. doi:10.1634/stemcells.2005-0503 [PubMed: 16690780]

Ono M, Yin P, Navarro A, Moravek MB, Coon VJS, Druschitz SA, Gottardi CJ, Bulun SE, 2014 Inhibition of canonical WNT signaling attenuates human leiomyoma cell growth. Fertil. Steril 101, 1441–1449.e1. doi:10.1016/j.fertnstert.2014.01.017 [PubMed: 24534281]

Ortiz-Pineda P. a, Ramírez-Gómez, F, Pérez-Ortiz J, González-Díaz S, Santiago-De Jesús F, Hernández-Pasos J, Del Valle-Avila C, Rojas-Cartagena C, Suárez-Castillo EC, Tossas K, Méndez-Merced AT, Roig-López JL, Ortiz-Zuazaga H, García-Arrarás JE, 2009 Gene expression profiling of intestinal regeneration in the sea cucumber. BMC Genomics 10, 262. doi: 10.1186/1471-2164-10-262 [PubMed: 19505337]

Osakada F, Ooto S, Akagi T, Mandai M, Akaike A, Takahashi M, 2007 Wnt signaling promotes regeneration in the retina of adult mammals. J. Neurosci 27, 4210–4219. doi:10.1523/JNEUROSCI.4193-06.2007 [PubMed: 17428999]

Pardo R, Andreolotti AG, Ramos B, Picatoste F, Claro E, 2003 Opposed effects of lithium on the MEK-ERK pathway in neural cells: Inhibition in astrocytes and stimulation in neurons by GSK3 independent mechanisms. J. Neurochem 87, 417–426. doi:10.1046/j.1471-4159.2003.02015.x [PubMed: 14511119]

Pasten C, Rosa R, Ortiz S, González S, García-Arrarás JE, 2012 Characterization of proteolytic activities during intestinal regeneration of the sea cucumber, Holothuria glaberrima. Int. J. Dev. Biol 56, 681–691. doi:10.1387/ijdb.113473cp [PubMed: 23319344]

Phiel CJ, Klein PS, 2001 Molecular targets of lithium action. Annu. Rev. Pharmacol. Toxicol 41, 789–813. doi:10.1146/annurev.pharmtox.41.1.789 [PubMed: 11264477]

Proffitt KD, Madan B, Ke Z, Pendharkar V, Ding L, Lee MA, Hannoush RN, Virshup DM, 2013 Pharmacological inhibition of the Wnt acyltransferase PORCN prevents growth of WNT-driven mammary cancer. Cancer Res. 73, 502–507. doi:10.1158/0008-5472.CAN-12-2258 [PubMed: 23188502]

Ramachandran R, Zhao X-F, Goldman D, 2011 Ascl1a/Dkk/beta-catenin signaling pathway is necessary and glycogen synthase kinase-3beta inhibition is sufficient for zebrafish retina regeneration. Proc. Natl. Acad. Sci. U. S. A 108, 15858–63. doi:10.1073/pnas.1107220108 [PubMed: 21911394]

Rhee J, Buchan T, Zukerberg L, Lilien J, Balsamo J, 2007 Cables links Robo-bound Abl kinase to N-cadherin-bound β-catenin to mediate Slit-induced modulation of adhesion and transcription. Nat. Cell Biol 9, 883–892. doi:10.1038/ncb1614 [PubMed: 17618275]

Rudolf A, Schirwis E, Giordani L, Parisi A, Lepper C, Taketo MM, Le Grand F, 2016 β-Catenin Activation in Muscle Progenitor Cells Regulates Tissue Repair. Cell Rep. 15, 1277–1290. doi: 10.1016/j.celrep.2016.04.022 [PubMed: 27134174]

Schacher S, Proshansky E, 1983 Neurite regeneration by Aplysia neurons in dissociated cell culture: modulation by Aplysia hemolymph and the presence of the initial axonal segment. J. Neurosci 3, 2403–2413. [PubMed: 6655493]

Smits VAJ, Essers MAG, Loomans DSE, Klompmaker R, Rijksen G, Medema RH, 1999 Inhibition of cell proliferation by lithium is associated with interference in cdc2 activation. FEBS Lett. 457, 23–27. doi:10.1016/S0014-5793(99)01002-9 [PubMed: 10486556]

Srivastava M, Mazza-Curll KL, Van Wolfswinkel JC, Reddien PW, 2014 Whole-body acoel regeneration is controlled by Wnt and Bmp-Admp signaling. Curr. Biol 24, 1107–1113. doi:10.1016/j.cub.2014.03.042 [PubMed: 24768051]

Stambolic V, Ruel L, Woodgett JR, 1996 Lithium inhibits glycogen synthase kinase-3 activity and mimics wingless signalling in intact cells. Curr. Biol 6, 1664–1668. doi:10.1016/S0960-9822(02)70790-2 [PubMed: 8994831]

Stoick-Cooper CL, Weidinger G, Riehle KJ, Hubbert C, Major MB, Fausto N, Moon RT, 2007 Distinct Wnt signaling pathways have opposing roles in appendage regeneration. Development 134, 479–489. doi:10.1242/dev.001123 [PubMed: 17185322]

Strand NS, Hoi KK, Phan TMT, Ray CA, Berndt JD, Moon RT, 2016 Wnt/B-catenin signaling promotes regeneration after adult zebrafish spinal cord injury. Biochem. Biophys. Res. Commun 477, 952–956. doi:10.1016/j.bbrc.2016.07.006 [PubMed: 27387232]

Sun LN, Yang HS, Chen MY, Xu DX, 2013 Cloning and expression analysis of Wnt6 and Hox6 during intestinal regeneration in the sea cucumber Apostichopus japonicus. Genet. Mol. Res 12, 5321–34. doi:10.4238/2013.November.7.7 [PubMed: 24301793]

Tanaka EM, Weidinger G, 2008 Heads or tails: can Wnt tell which one is up? Nat. Cell Biol 10, 122–124. doi:10.1038/ncb0208-122 [PubMed: 18246038]

Teo JL, Kahn M, 2010 The Wnt signaling pathway in cellular proliferation and differentiation: A tale of two coactivators. Adv. Drug Deliv. Rev 62, 1149–1155. doi:10.1016/j.addr.2010.09.012 [PubMed: 20920541]

Velloso CP, Kumar A, Tanaka EM, Brockes JP, 2000 Generation of mononucleate cells from post-mitotic myotubes proceeds in the absence of cell cycle progression. Differentiation 66, 239–246. doi:10.1046/j.1432-0436.2000.660410.x [PubMed: 11269950]

Wang Z, Zhang X, Chen S, Wang D, Wu J, Liang T, Liu C, 2013 Lithium Chloride Inhibits Vascular Smooth Muscle Cell Proliferation and Migration and Alleviates Injury-Induced Neointimal Hyperplasia via Induction of PGC-1α. PLoS One 8. doi:10.1371/journal.pone.0055471

Wehner D, Cizelsky W, Vasudevaro M, Özhan G, Haase C, Kagermeier-Schenk B, Röder A, Dorsky RI, Moro E, Argenton F, Kühl M, Weidinger G, 2014 Wnt/β-catenin signaling defines organizing centers that orchestrate growth and differentiation of the regenerating zebrafish caudal fin. Cell Rep. 6, 467–481. doi:10.1016/j.celrep.2013.12.036 [PubMed: 24485658]

Whyte JL, Smith a. a., Helms J. a., 2012 Wnt Signaling and Injury Repair. Cold Spring Harb. Perspect. Biol 4, a008078–a008078. doi:10.1101/cshperspect.a008078

Yan M, Li G, An J, 2017 Discovery of small molecule inhibitors of the Wnt/β-catenin signaling pathway by targeting β-catenin/Tcf4 interactions. Exp. Biol. Med 242, 1185–1197. doi:10.1177/1535370217708198

Yokoyama H, Ogino H, Stoick-Cooper CL, Grainger RM, Moon RT, 2007 Wnt/β-catenin signaling has an essential role in the initiation of limb regeneration. Dev. Biol 306, 170–178. doi:10.1016/j.ydbio.2007.03.014 [PubMed: 17442299]

Yuan J, Gao Y, Sun L, Jin S, Zhang X, Liu C, Li F, Xiang J, 2019 Wnt Signaling Pathway Linked to Intestinal Regeneration via Evolutionary Patterns and Gene Expression in the Sea Cucumber Apostichopus japonicus. Front. Genet 10, 1–13. doi:10.3389/fgene.2019.00112 [PubMed: 30804975]

Zhao J, Morozova N, Williams L, Libs L, Avivi Y, Grafi G, 2001 Two phases of chromatin decondensation during dedifferentiation of plant cells. Distinction between competence for cell fate switch and a commitment for S phase. J. Biol. Chem 276, 22772–22778. doi:10.1074/jbc.M101756200 [PubMed: 11274191]

Zhou YX, Shi Z, Singh P, Yin H, Yu Y. ni, Li L, Walsh MP, Gui Y, Zheng XL, 2016 Potential Role of Glycogen Synthase Kinase-3β in Regulation of Myocardin Activity in Human Vascular Smooth Muscle Cells. J. Cell. Physiol 231, 393–402. doi:10.1002/jcp.25084 [PubMed: 26129946]

Zhu J, Burke AK, Del Rio-Tsonis K, Haynes T, Zavada J, Luz-Madrigal A, 2014 β-Catenin Inactivation Is a Pre-Requisite for Chick Retina Regeneration. PLoS One 9, e101748. doi:10.1371/journal.pone.0101748 [PubMed: 25003522]

## Highlights

- LiCl, an alleged activator of Wnt pathway, enhances the formation of the intestinal rudiment while treatment with iCRT14, a putative antagonist of Wnt signaling, causes a reduction in the size of the rudiment
- During early intestinal regeneration in *Holothuria glaberrima* cell proliferation appears to be mediated by the canonical Wnt signaling pathway while muscle dedifferentiation appears to be mediated by a Wnt-independent signaling via GSK-3
- Cell dedifferentiation can be decoupled from cell proliferation during intestinal regeneration in *H. glaberrima*

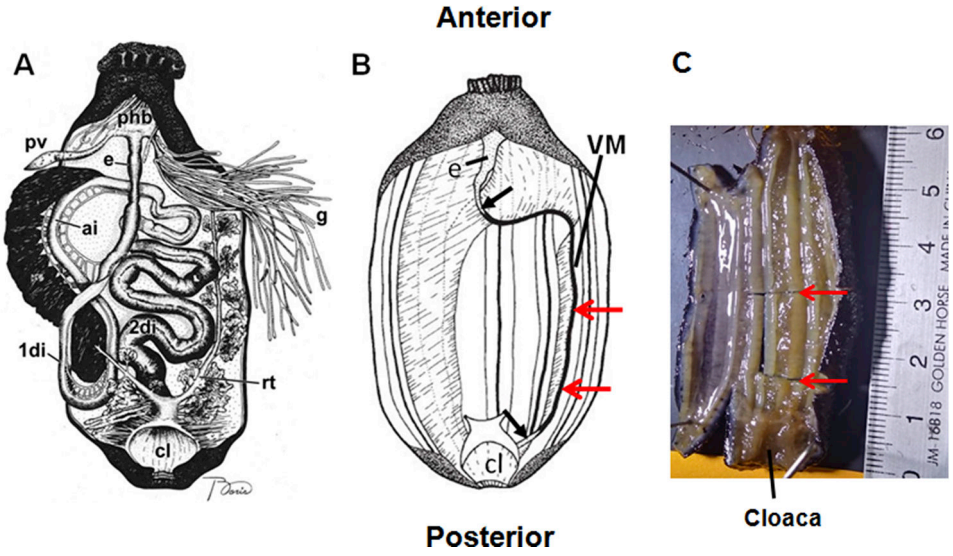


**Figure 1. Diagram illustrating visceral anatomy before and after evisceration.**

The animal is positioned with the anterior end to the top. Before evisceration the digestive tract is composed of the esophagus (e), first descending intestine (1di), ascending intestine (ai), second descending intestine (2di), and the cloaca (cl). Other organs shown are: gonads (g), pharyngeal bulb (phb), polian vesicle (Pv), and respiratory tree (rt) **(A)**. During evisceration most of the internal organs are ejected through the cloaca, only remaining a segment of the esophagus (e), the cloaca (cl), and the mesenteries. From the distal end of the ventral mesentery (VM) a new intestine develops. Black arrows point out to the forming intestine connections to the esophagus and cloaca. Red arrows indicate the segment of the regenerating mesentery dissected and used for histological studies in *in vivo* studies **(B)**. A photograph of a sea cucumber where a segment (red arrows) of the body wall with attached regenerating mesentery has been dissected to be embedded in OCT for cryosectioning is shown **(C)**. Diagrams are not to scale and were modified from (Mashanov and García-Arrarás, 2011; and García-Arrarás et al., 1998)

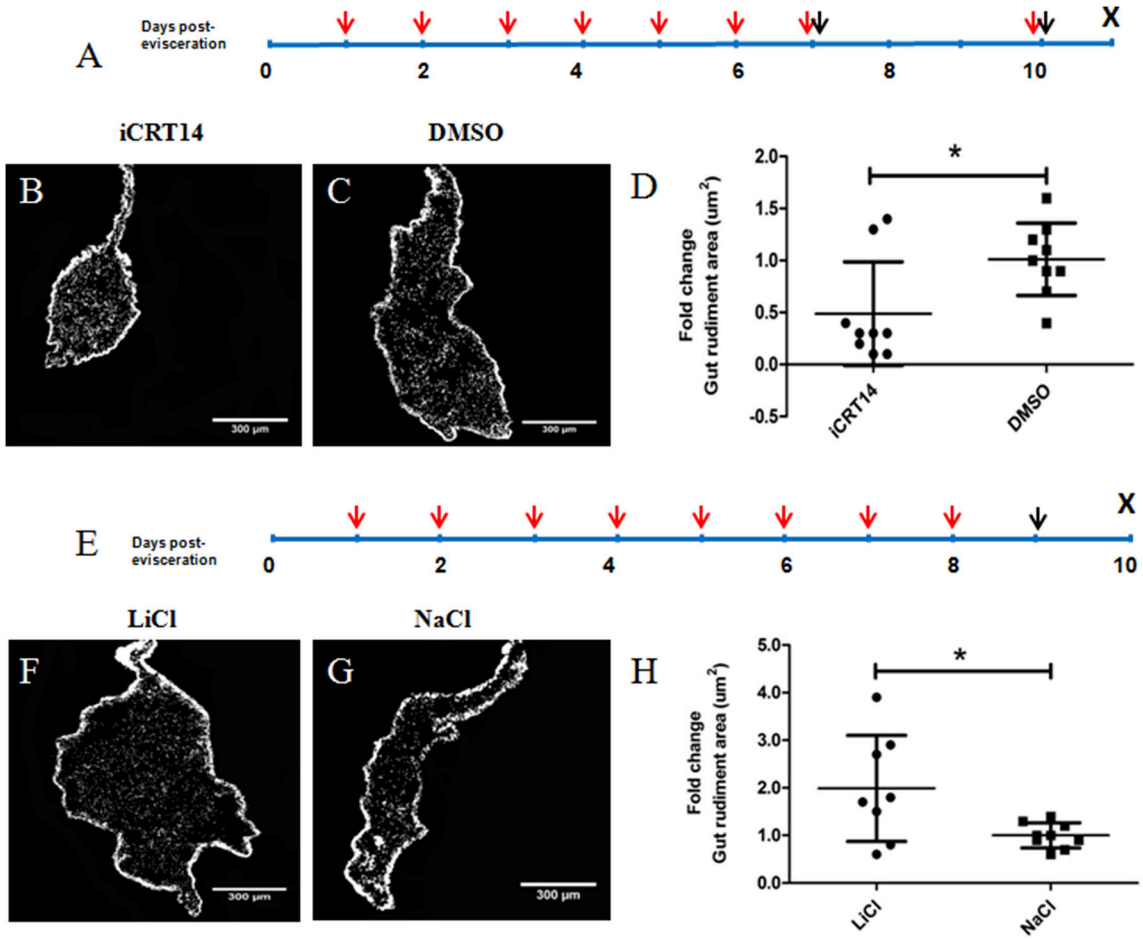


**Figure 2. Effects of iCRT14 and LiCl treatments on the size of the regenerating gut rudiment *in vivo*.**

Schematic diagrams depicting the experimental protocol used for iCRT14 **(A)** or LiCl **(E)** treatment *in vivo*. Red arrows indicate the time points when the putative Wnt pathway antagonist (iCRT14) or the presumed Wnt pathway agonist (LiCl) were injected intracoelomically, black arrows indicate when the BrdU was injected, and X when the animals were sacrificed. Representative histological cross sections of intestines and attached mesenteries showing the effect of iCRT14 **(B)** and LiCl **(F)** treatment on gut rudiment size compared to the controls DMSO **(C)** and NaCl **(G)**, respectively. Treatment with iCRT14 leads to a significant reduction in the gut rudiment area compared to controls **(D)**. Conversely, treatment with LiCl results in a significant increase in the gut rudiment area compared to controls **(H)**. Results represent the mean ± SD, t-test, *$p<0.05$, n= 9 iCRT14, n = 9 DMSO, n = 8 LiCl, n = 9 NaCl. Scale bars = 300 µm.

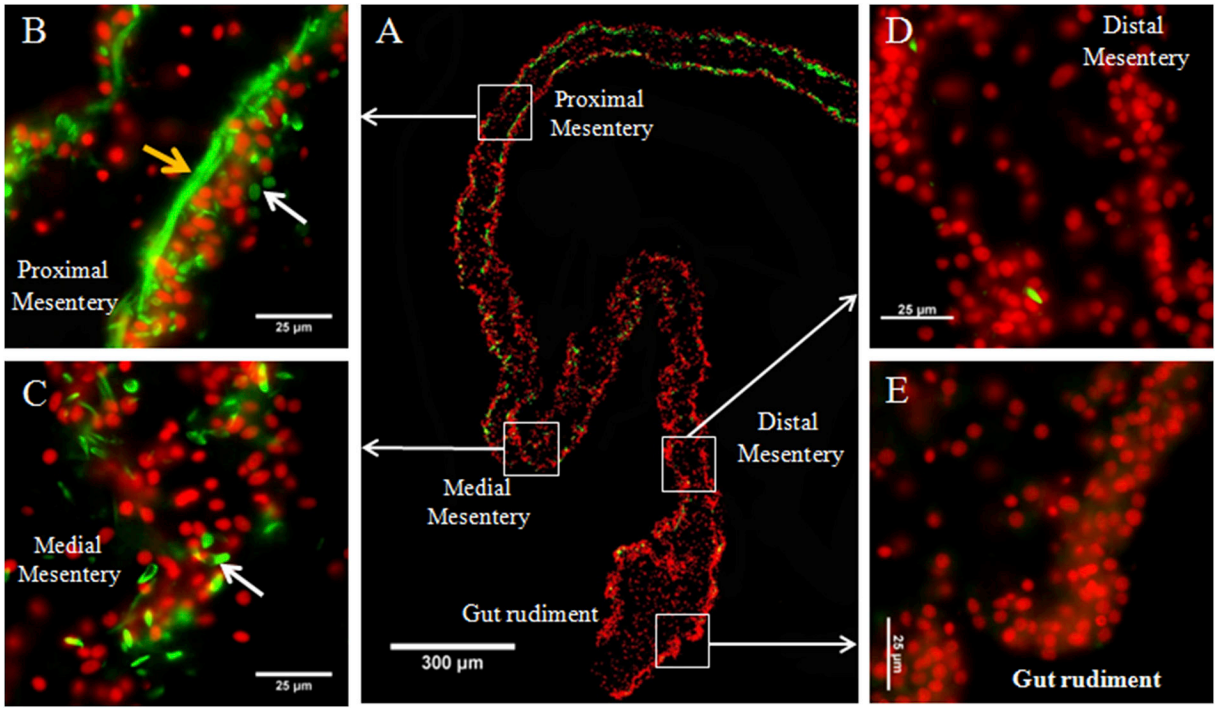


**Figure 3. Spindle-like structures (SLSs) and muscle fibers gradient in regenerating intestines in *H. glaberrima*.**

Representative histological cross sections of a gut rudiment and the attached mesentery showing the gradient of SLSs and muscle fibers observed during early stages of intestine regeneration. The whole gut rudiment and adjacent mesentery is shown in **(A)**. At higher magnification are shown the proximal (**B**), medial **(C)**, and distal mesentery **(D)**, as well as the gut rudiment **(E)**. Muscle fibers (yellow arrows) are observed in proximal mesentery and SLSs (white arrows) are observed in both proximal and medial mesentery. Conversely, no SLSs or muscle fibers are present in distal mesentery and gut rudiment. SLSs and muscle fibers are shown in green (Phalloidin-TRITC) and cell nuclei in red (DAPI). Scale bars = 300 µm in **(A)** and 25 µm in **(B)**, **(C)**, **(D)**, and **(E)**.

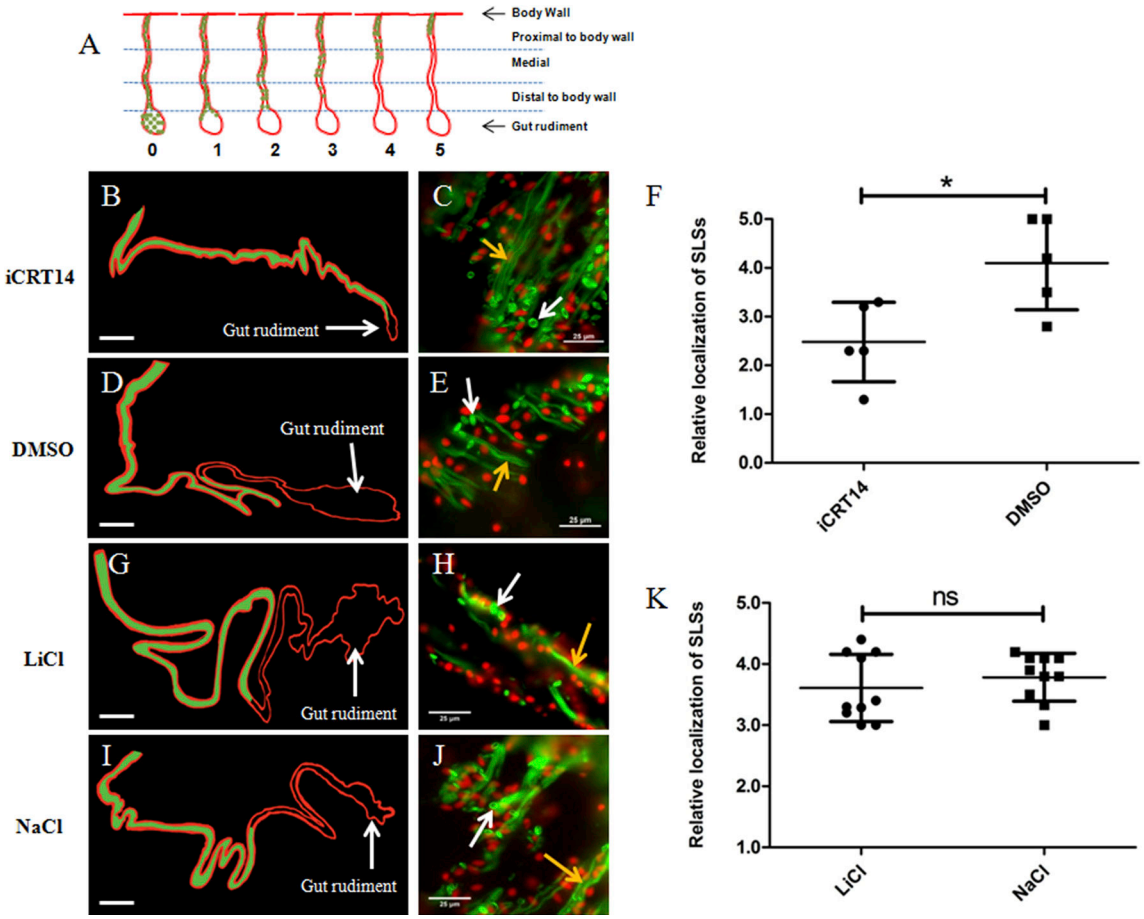


**Figure 4. Effect of iCRT14 on mesentery muscle dedifferentiation *in vivo*.**

**(A)** Diagram that depicts the staging system used for quantifying mesenterial muscle dedifferentiation *in vivo*. Stages are based on the localization of the SLSs in the mesentery relative to the body wall and the gut rudiment. Representative histological cross sections of gut rudiments and attached mesenteries showing the effects of iCRT14 **(B)** and LiCl **(G)** treatments on mesenterial muscle dedifferentiation compared to controls DMSO **(D)** and NaCl (**I**), respectively are shown. The areas of the mesentery where SLSs were observed in the different tissues are presented in green in the schemes for clarity purposes **(B,D,G,I)**. SLSs were observed adjacent to the gut rudiment in iCRT14-treated animals **(B)** while they were localized in the middle segment of the mesentery in control animals (DMSO-treated) (**D**). Furthermore, SLSs were observed in the middle segment of the mesentery in both LiCl (**G**) and NaCl **(I)** treated groups. The micrographs on the right **(C,E,H,J)** show the presence of SLS (white arrows) and muscle fibers (yellow arrows) in the different samples. A significant difference in the localization of SLSs was found between iCRT14 -treated animals and controls, suggesting a delay in muscle dedifferentiation due to iCRT14 treatment **(F)**. Conversely, no significant differences were found between LiCl and control **(K)**. Results represent the mean ± SD, t-test, *$p<0.05$, n= 5 iCRT14, n =5 DMSO, n= 10 LiCl, n= 10 NaCl. SLSs and muscle fibers are shown in green (Phalloidin-TRITC) and cell nuclei in red (DAPI). The gut rudiment is pointed out in the schemes of the tissue sections. The schemes were drawn to scale. Scale = 300 μm **(B,D,G,I)** and 25 μm **(C,E,H,J)**.

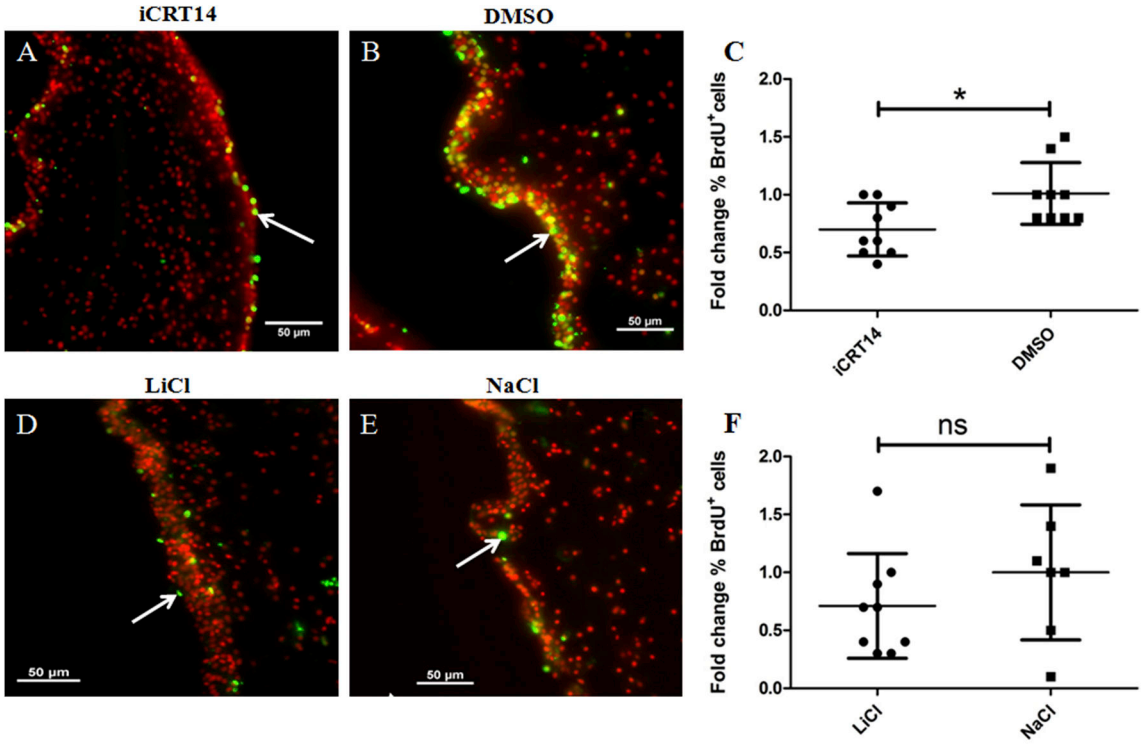


**Fig 5. iCRT14 but not LiCl alter cell proliferation during intestine regeneration *in vivo*.**

Cell proliferation was assayed by BrdU incorporation. Representative histological cross sections of gut rudiments showing the effect of iCRT14 **(A)** and LiCl **(D)** treatments on cell proliferation compared to controls DMSO **(B)** and NaCl **(E)**, respectively. iCRT14 reduces significantly the percentage of BrdU labeled cells compared to controls (DMSO) **(C)**. However, no significant differences in the percentage of BrdU labeled cells were found between LiCl-treated animals and their controls NaCl (**F**). Results represent the mean ± SD, t-test, *$p<0.05$, n = 9 iCRT14, n = 9 DMSO, n = 9 LiCl, n = 7 NaCl. Cell nuclei are shown in red (DAPI) and $BrdU^+$ nuclei (white arrows) in green. Scale bar = 50 µm.

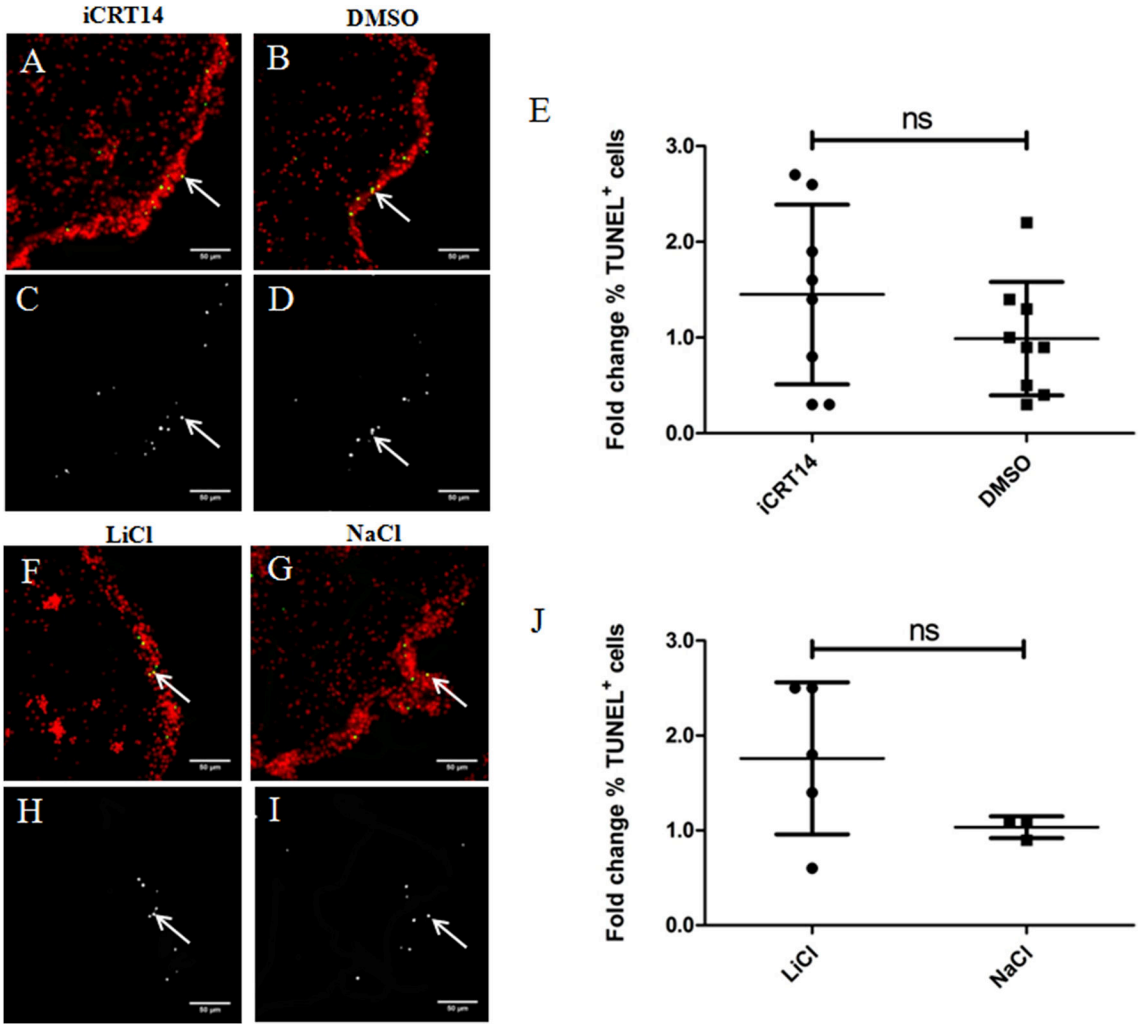


**Fig. 6. Neither iCRT14 nor LiCl show any effect on apoptosis during intestine regeneration.**

Programmed cell death was measured using TUNEL. Representative histological cross sections of gut rudiments showing the effect of iCRT14 **(A,C)** and LiCl **(F,H)** treatments on programmed cell death compared to controls DMSO **(B,D)** and NaCl **(G,I)**, respectively. No significant differences in the percentage of TUNEL labeled cells were found between iCRT14-treated or LiCl-treated animals and their respective controls DMSO and NaCl (**E** and **J**, respectively). Results represent the mean ± SD, t-test, n = 8 iCRT14, n = 9 DMSO, n = 5 LiCl, n = 3 NaCl. The micrographs on the bottom **(C,D,H,I)** show the TUNEL labeled nuclei in white. Micrographs on the top **(A,B,F,G)** show the cell nuclei in red (DAPI) and TUNEL labeled nuclei (white arrows) in green. Scale bar = 50 μm.

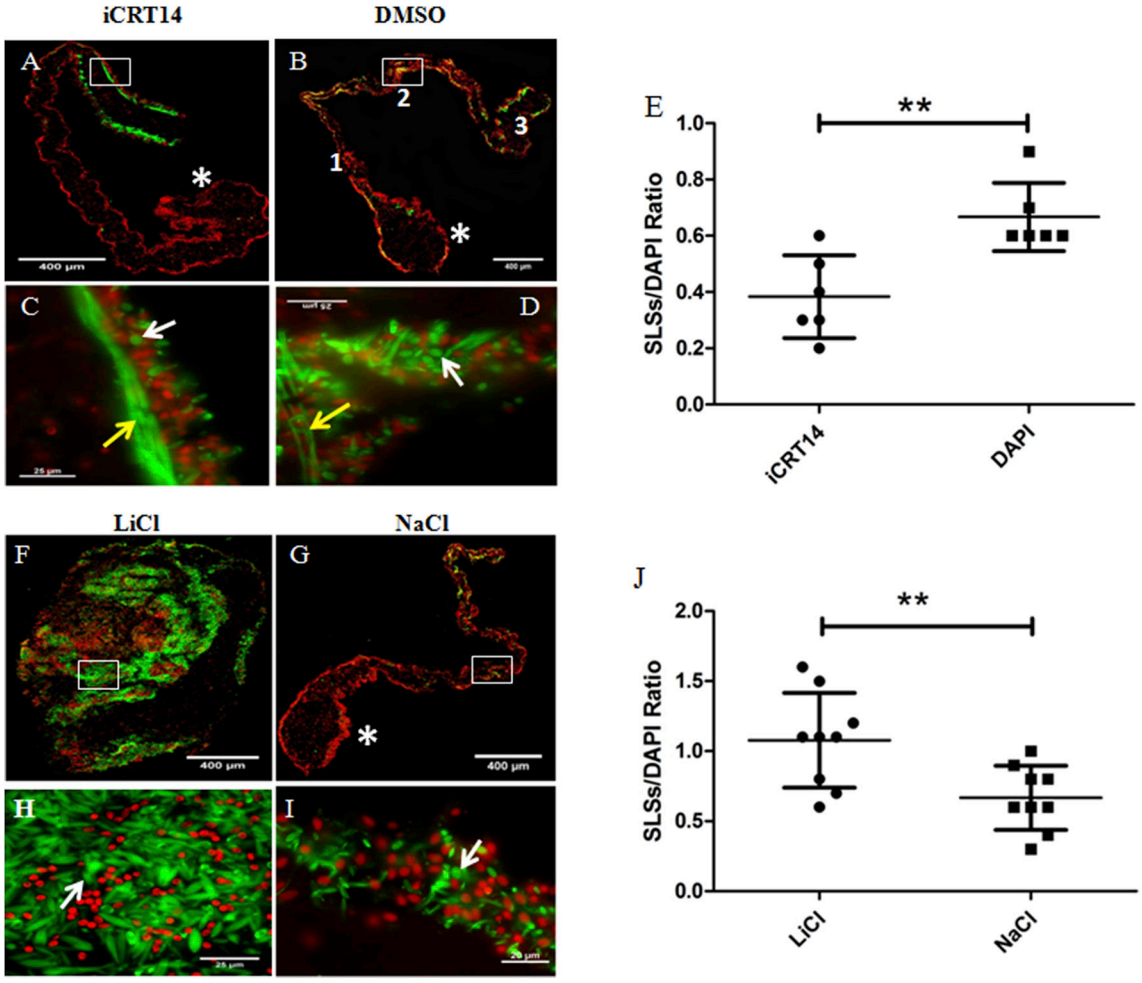


**Figure 7. Effect of iCRT14 and LiCl on muscle dedifferentiation *in vitro*.**

SLS/DAPI ratio was determined as an indicator of muscle dedifferentiation. Representative histological cross sections of explants showing the effect of iCRT14 **(A,C)** and LiCl **(F,H)** treatment on muscle dedifferentiation and tissue morphology compared to controls DMSO **(B,D)** and NaCl **(G,I)**, respectively. LiCl-treated explants lose their characteristic gut rudiment and mesentery organization **(F)** compared to controls **(G)**. The micrographs on the bottom **(C,D,H,I)** are high-magnification view of the boxed regions in the micrographs on the top (**A,B,F,G**, respectively). iCRT14 treatment reduces significantly the SLS/DAPI ratio compared to controls **(E)**. Conversely, the SLS/DAPI ratio was significantly greater in LiCl-treated explants compared to controls **(J)**. Results represent the mean ± SD, t-test, **p<0.01, n = 6 iCRT14, n = 6 DMSO, n = 9 LiCl, n = 9 NaCl. SLSs (white arrows) and muscle fibers (yellow arrows) are shown in green (phalloidin-TRITC) and cell nuclei in red (DAPI). The gut rudiments are indicated in the micrographs by asterisks. The regions of the mesentery where the SLSs and cell nuclei were counted are indicated by numbers in **(B): 1**= near the gut rudiment; **2**= medial segment; and **3**= near the body wall. Scale bar = 400 µm **(A,B,F,G)**, 25 µm **(C,D,H,I)**.

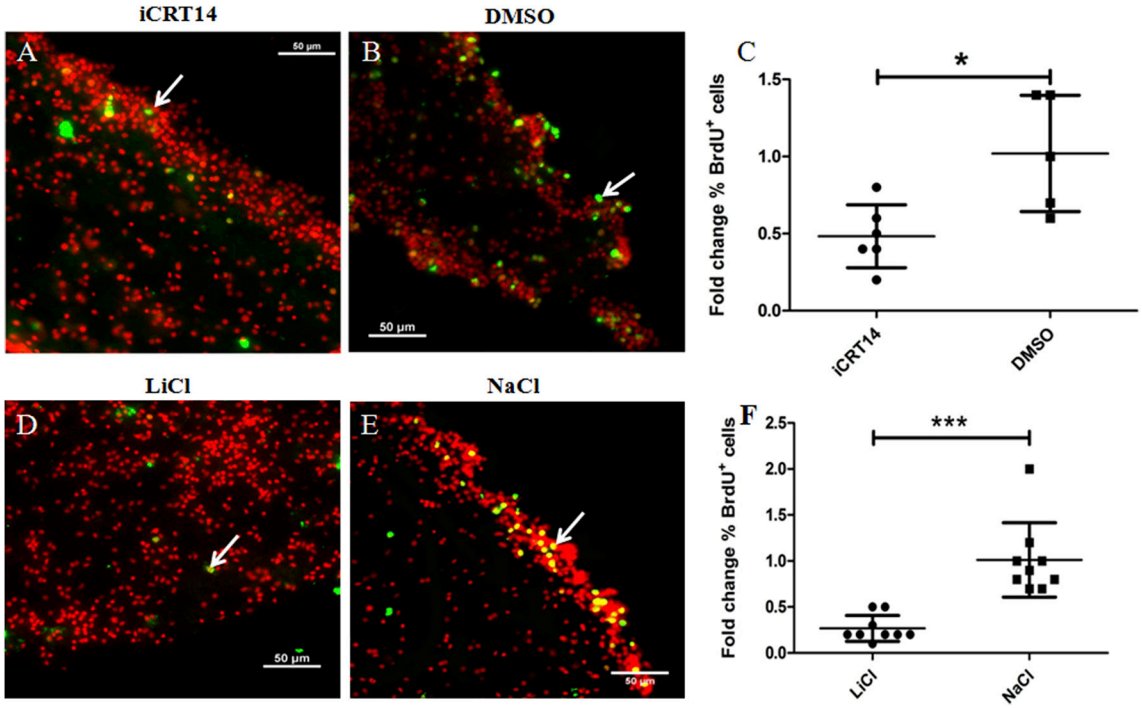


**Figure 8. Both iCRT14 and LiCl reduce cell proliferation *in vitro*.**

Cell proliferation was assayed by BrdU incorporation. Representative histological cross sections of explants showing the effect of iCRT14 **(A)** and LiCl **(D)** treatments on cell proliferation compared to controls DMSO **(B)** and NaCl **(E)**, respectively. Both iCRT14 and LiCl treatments resulted in a significant reduction in the percentage of BrdU labeled cells in explants compared to controls (DMSO and NaCl) (**C and F**, respectively). Results represent the mean ± SD, t-test, * $p<0.05$, ***$p<0.001$, n = 6 iCRT14, n = 5 DMSO, n = 9 LiCl, n = 9 NaCl. Cell nuclei are shown in red (DAPI) and $BrdU^+$ nuclei (white arrows) in green. Scale bar = 50 µm.

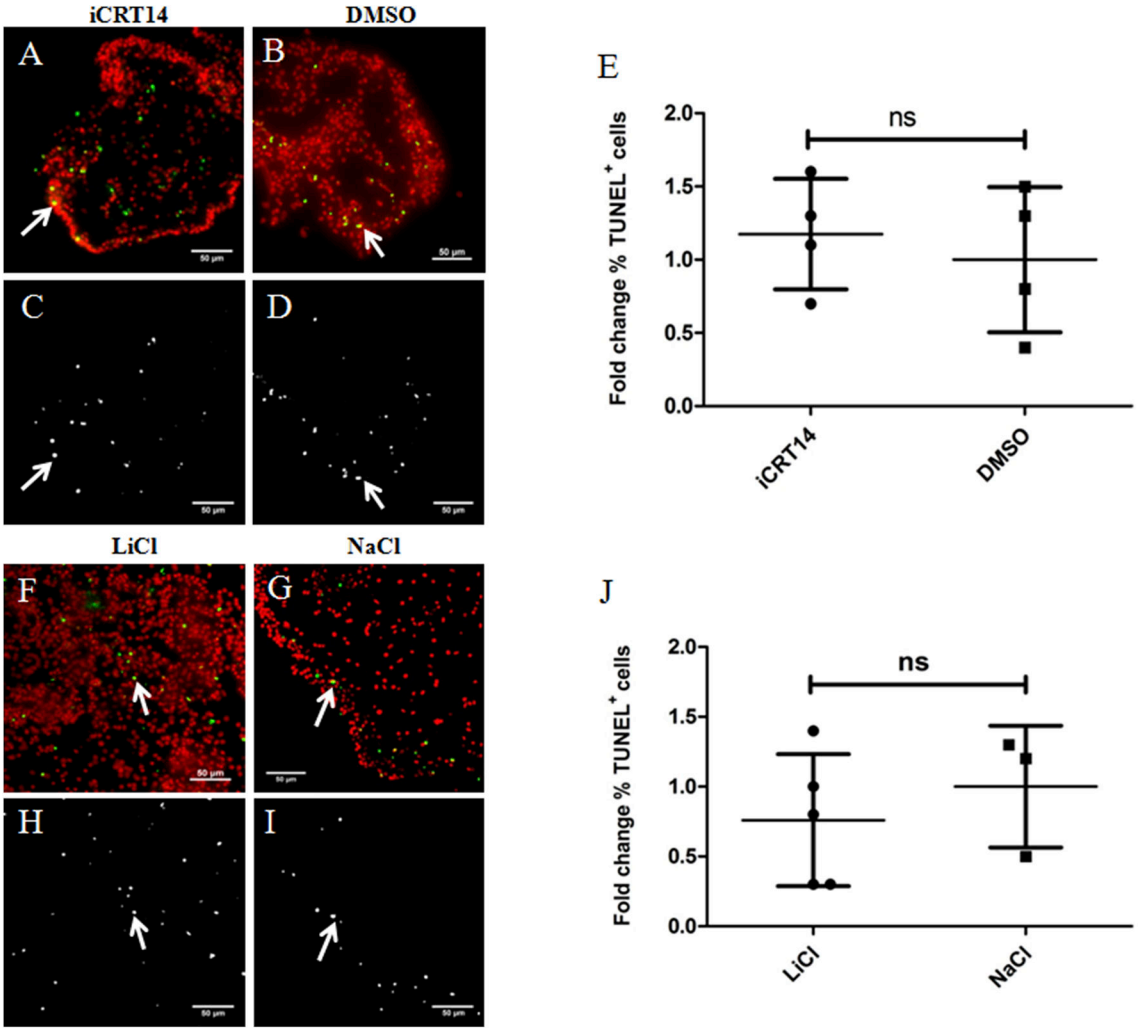


**Fig. 9. Neither iCRT14 nor LiCl alter apoptosis *in vitro*.**

Programmed cell death was evaluated using TUNEL. Representative histological cross sections of gut explants showing the effect of iCRT14 **(A,C)** and LiCl **(F,H)** treatments on cell proliferation compared to controls DMSO **(B,D)** and NaCl **(G,I)**, respectively. No significant differences in the percentage of TUNEL labeled nuclei were found between iCRT14-treated or LiCl-treated explants and their respective controls DMSO and NaCl (**E** and **J**, respectively). Results represent the mean ± SD, t-test, n = 4 iCRT14, n = 4 DMSO, n = 5 LiCl, n = 3 NaCl. The micrographs on the bottom **(C,D,H,I)** show TUNEL labeled nuclei (white arrows) in white. Micrographs on the top **(A,B,F,G)** show the cell nuclei in red (DAPI) and TUNEL labeled nuclei (white arrows) in green. Scale bar = 50 μm.

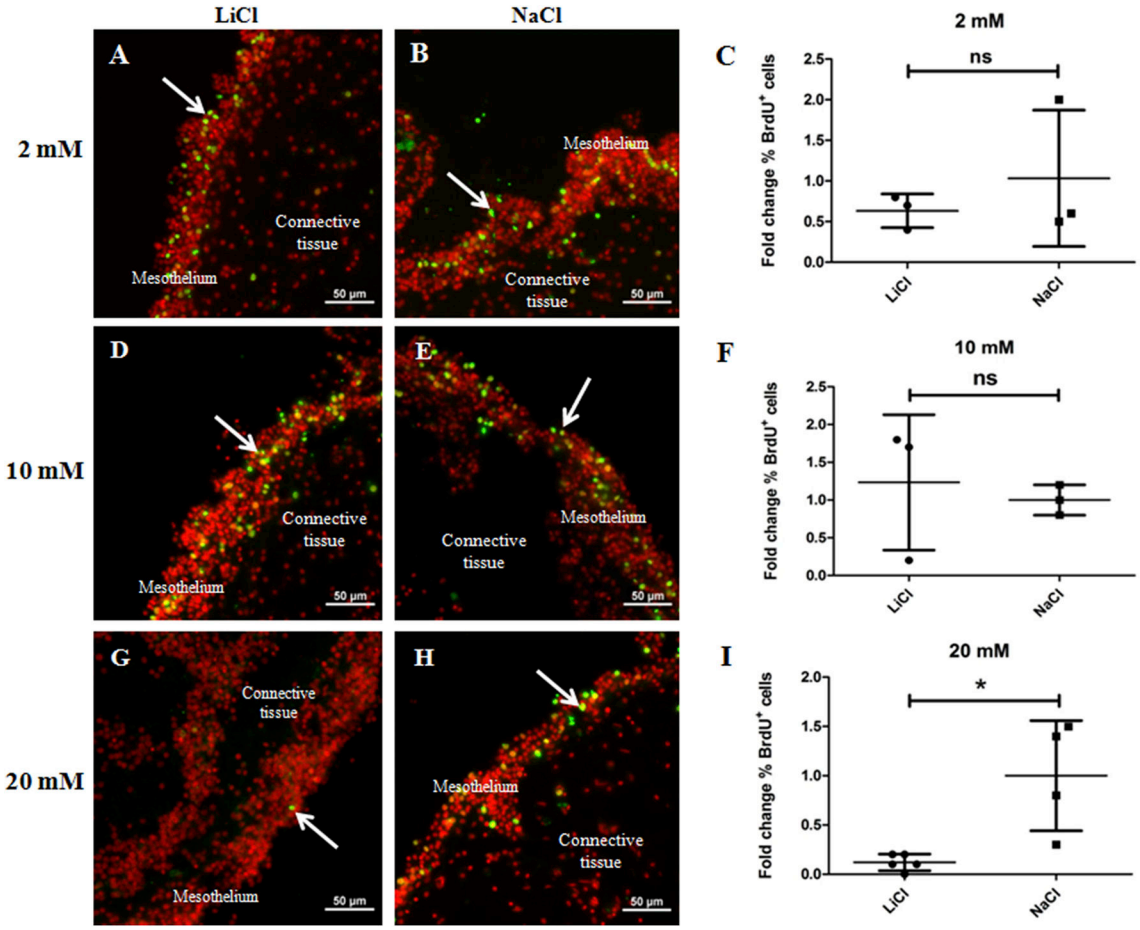


**Figure 10. 20 mM LiCl reduces mesothelial cell proliferation in gut rudiment explants from 14 dpe animals.**

Cell proliferation was assayed by BrdU incorporation. Representative histological cross sections of explants showing the effect of LiCl at 2 mM **(A)**, 10 mM **(D)**, and 20 mM **(G)** and their respective controls: 2 mM **(B)**, 10 mM **(E)**, and 20 mM **(H)** NaCl on mesothelial cell proliferation. LiCl doses of 2 mM and 10 mM did not have significant effects on the percentage of BrdU labeled cells in the mesothelium compared to controls (2 mM and 10 mM NaCl-treated explants) (**C** and **F**, respectively). However, 20 mM LiCl treatment resulted in a significant reduction in the percentage of $BrdU^+$ cells in the mesothelium compared to controls (20 mM NaCl-treated explants) **(I)**. Results represent the mean ± SD, t-test, * $p<0.05$, n = 3 in 2mM and 10 mM LiCl, n = 3 in 2 mM and 10 mM NaCl, n = 5 in 20 mM LiCl, n = 4 in 20 mM NaCl. Cell nuclei are shown in red (DAPI) and BrdU labeled nuclei (white arrows) in green. Scale bar = 50 µm.

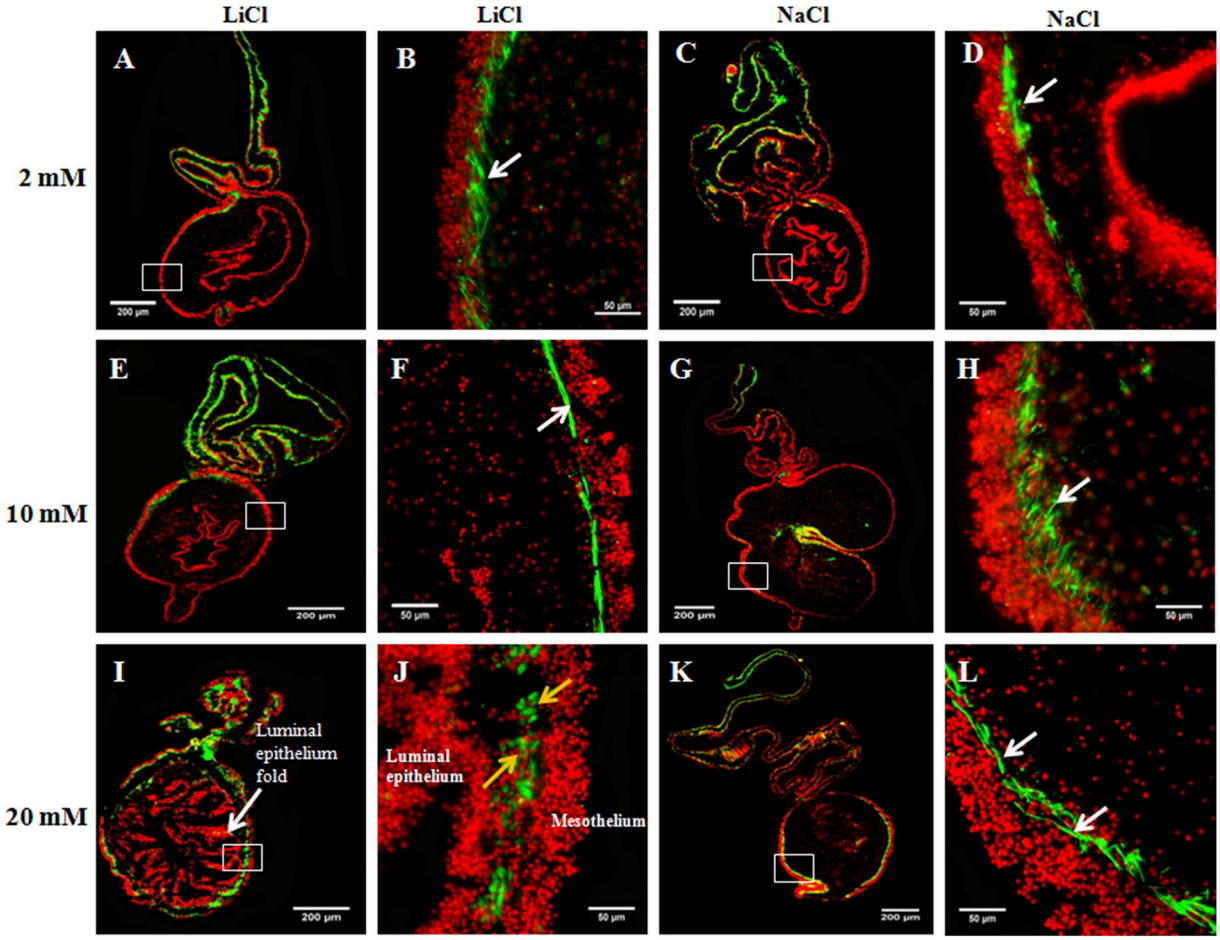


**Figure 11. 20 mM LiCl induces muscle dedifferentiation in gut rudiment explants from 14 dpe animals.**

The ability of LiCl at three doses (2, 10, and 20 mM) to promote gut rudiment muscle dedifferentiation was tested in explants from 14 dpe. Representative histological cross sections of intestines and attached mesenteries showing the effect of LiCl at 2 mM **(A,B)**, 10 mM **(E,F)**, and 20 mM **(I,J)** and their respective controls: 2 mM **(C,D)**, 10 mM **(G,H)**, and 20 mM **(K,L)** NaCl. Explants treated with 2 mM LiCl **(B)** or 10 mM LiCl **(F)** showed a muscle layer similar to those observed in control explants, 2 mM NaCl **(D)** and 10 mM NaCl **(H)**. Moreover, these explants had similar morphology (**A** and **E**, respectively) to control explants (**C** and **G**, respectively). However, explants treated with 20 mM showed SLSs and small spherical cells instead of a defined muscle layer **(J)**. These explants also presented altered tissue morphology with abundant luminal epithelium folds and a reduced connective tissue space **(I)**. Conversely, control explants (treated with 20mM NaCl) showed a defined muscle layer in the gut rudiment **(L)** and typical explant morphology **(K)**. The micrographs on the first **(A,E,I)** and third column **(C,G,K)** show the LiCl and NaCl-treated explant morphology, respectively, at low magnification. The micrographs on the second and fourth columns show the gut rudiment muscle layer (white arrows) or SLSs (yellow arrows) at higher magnification in LiCl and NaCl-treated explants, respectively, in green. Cell nuclei (DAPI) are shown in red. The mesothelium and luminal epithelium are pointed out in 20

mM LiCl treated explants **(I,J)**. n = 4. Scale bar = 200 μm **(A,E,I,C,G,K)** and 50 μm **(B,F,J,D,H,L)**.

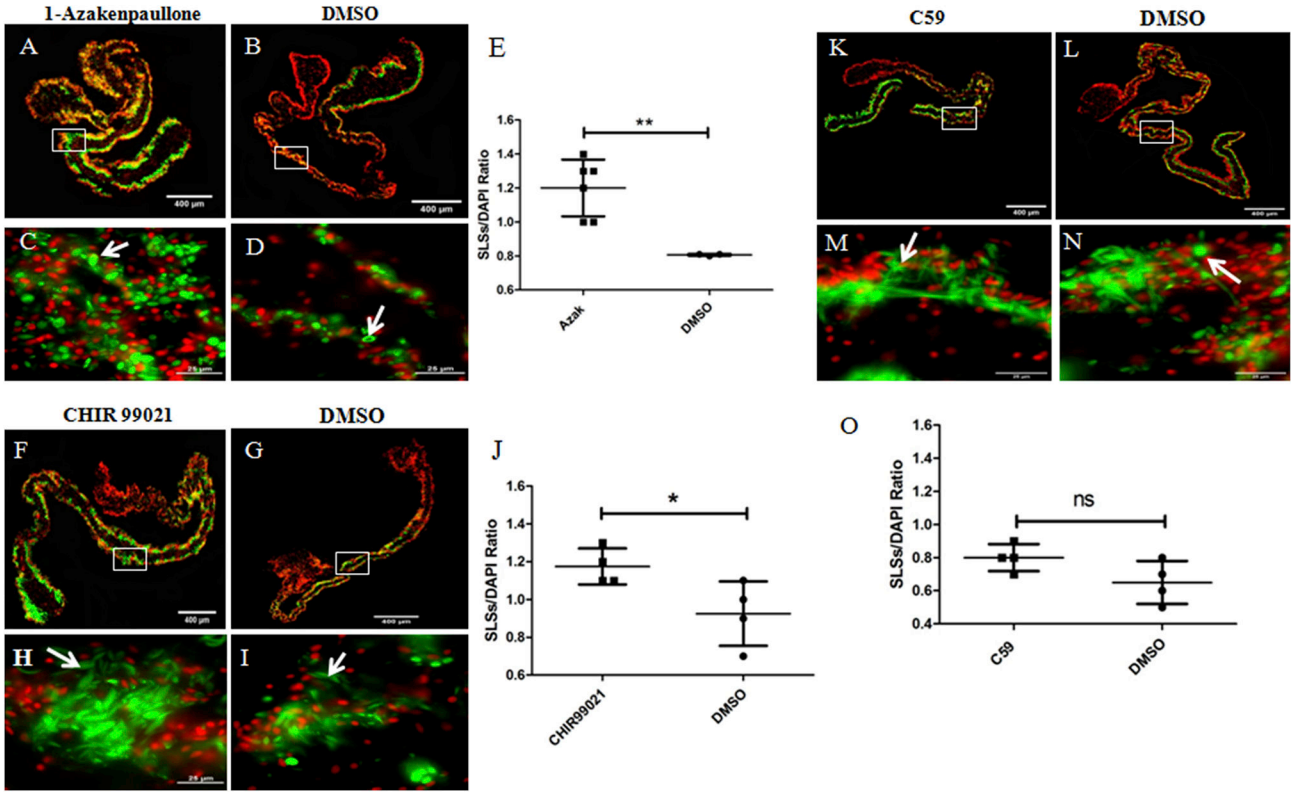


**Figure 12. Effects of known GSK-3 inhibitors and C59 on muscle dedifferentiation *in vitro*.**

The SLSs/DAPI ratios in explants treated with the GSK-3 inhibitors 1-Azakenpaullone and CHIR99021, and the Wnt antagonist C59, were measured as indicators of muscle dedifferentiation. Representative histological cross sections of explants showing the effect of 1-Azakenpaullone **(A,C)**, CHIR99021 **(F,H)**, C59 **(K,M)** and their controls **(B,D), (G,I)**, and **(L,N)**, respectively. The micrographs on the bottom **(C,D,H,I,M,N)** are high-magnification view of the boxed regions in the top micrographs (**A,B,F,G**,**K,L** respectively). Both 1-Azakenpaullone **(E)** and CHIR99021 treatment **(J)** increased significantly the SLSs/DAPI ratio compared to controls. Conversely, we did not find significant differences in the SLS/DAPI ratio between C59 treated explants and their controls (DMSO) **(O)**. Results represent the mean ± SD, t-test, **p<0.01, *p<0.05, n = 6 Azakenpaullone, n = 4 CHIR99021, n = 4 C59, n = 3–4 DMSO. SLSs (white arrows) are shown in green (phalloidin-TRITC) and cell nuclei in red (DAPI). Scale bar = 400 μm **(A,B,F,G,K,L)**, 25 μm **(C,D,H,I,M,N)**.

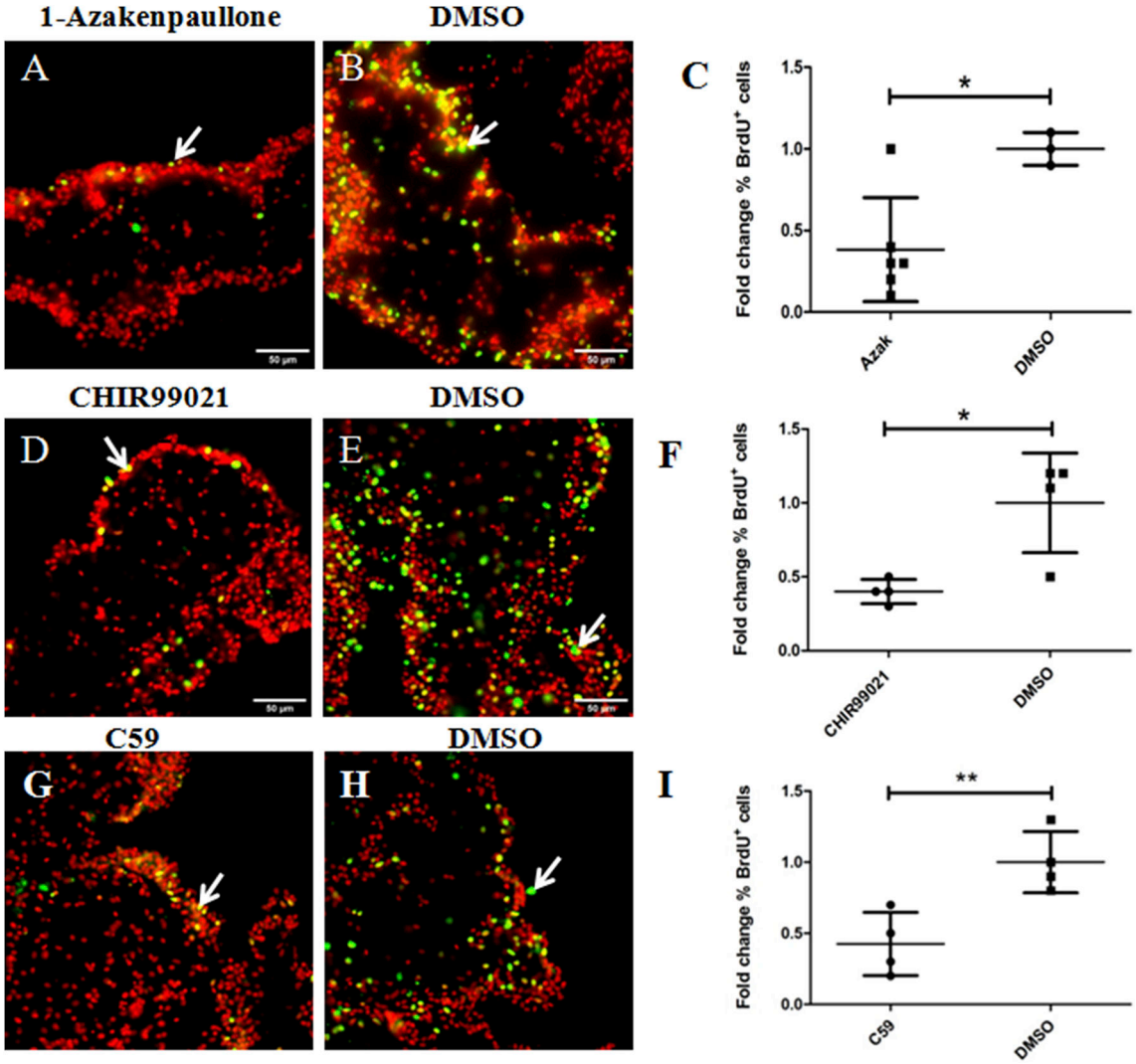


**Figure 13. Effects of known GSK-3 inhibitors and C59 on cell proliferation *in vitro*.**

Cell proliferation was assayed by BrdU incorporation. Representative histological cross sections of explants showing the effect of 1-Azakenpaullone **(A)**, CHIR99021 **(D)**, and C59 **(G)** treatments compared to controls DMSO **(B), (E)**, and **(H)**, respectively. We found that both GSK-3 inhibitors **(**1-Azakenpaullone and CHIR99021) as well as C59 treatments result in a significant reduction in the percentage of BrdU labeled cells in explants compared to controls DMSO (**C, F**, and **I**, respectively). Results represent the mean ± SD, t-test, * $p<0.05$, ** $p<0.01$, n = 6 1-Azakenpaullone (AZAK), n = 4 CHIR99021, n = 4 C59, n = 3–4 DMSO. Cell nuclei are shown in red (DAPI) and BrdU labeled nuclei (white arrows) in green. Scale bar = 50 μm

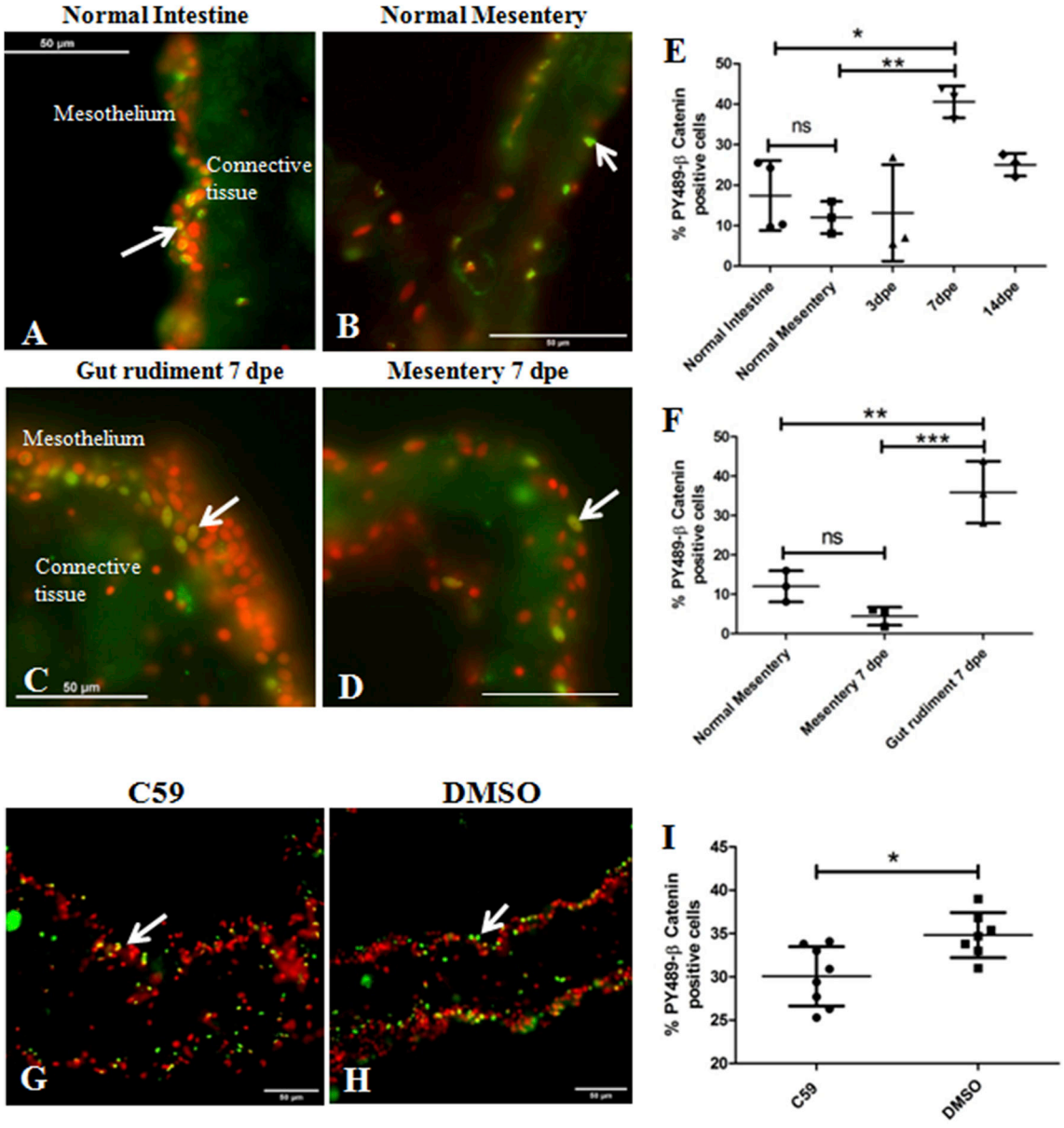


**Figure 14. *In vivo* and *in vitro* expression of PY489-β-catenin.**

Activation of the Canonical β-catenin pathway in normal and regenerating intestines was determined *in vivo* **(A-F)** and *in vitro* **(G-I)** by immunohistochemistry using the monoclonal antibody Anti-PY489-β-catenin to detect its nuclear expression, a proxy for β -catenin activation. Representative histological cross sections of normal intestinal mesothelium **(A)**, normal mesentery **(B)**, gut rudiments at 7 dpe **(C)** and regenerating mesentery at 7 dpe **(D)** show the nuclear labeling of the antibody to be mainly in some mesothelial cells. A significant increase in the percentage of mesothelial cell nuclei labeled with the PY489-β-catenin antibody was observed at 7 dpe compared to the normal intestine and mesentery **(E)**. The increase in PY489-β-catenin immunoreactive cell nuclei was localized to the gut rudiment; no significant differences in the percentage was observed between normal mesentery and regenerating mesentery at 7 dpe **(F)**. Results represent the mean ± SD, One-

Way ANOVA, * $p<0.05$, *$p<0.01$, n = 3–4. Treatment of *in vitro* explants with C59 reduced nuclear β-catenin expression. Representative histological cross sections of gut explants treated with C59 **(G)** and its control (DMSO) **(H)**. C59 caused a significant reduction in the percentage of PY489-β-catenin labeled cell nuclei compared to controls (DMSO), suggesting that this drug inhibits the Wnt pathway in gut explants **(I)**. Results represent the mean ± SD, t-test, * $p<0.05$, n = 8 for C59, n = 7 for DMSO. Cell nuclei are shown in red (DAPI) and PY489-β-catenin labeled nuclei (white arrows) in green. Scale bar = 50 μm.

**Table 1.**

Effects of putative canonical Wnt signaling pathway modulators on cell proliferation, muscle dedifferentiation and apoptosis in intestine explants after 72h of treatment *in vitro*

| Compound | Dose(s) in μM unless otherwise stated | Target | Effect on Wnt signaling | Effects on intestine explants | | | Reference(s) |
|---|---|---|---|---|---|---|---|
| | | | | Cell proliferation | Muscle dedifferentiation | Apoptosis | |
| LiC1 | 20 mM | GSK-3 | Activates | ↓ **(70%)** | ↑ **(169%)** | → | (Klein and Melton, 1996) |
| | 10 mM | | | → | ↑ | ND | |
| | 2 mM | | | → | → | ND | |
| 1- Azaken paullone | 100–20 * | GSK-3 | Activates | ↓ **(60%)** | ↑ **(50%)** | ND | (Kunick et al., 2004) |
| | 2 | | | → | → | ND | |
| CHIR99021 or CT99021 | 20 | GSK-3 | Activates | ↓ **(60%)** | ↑ **(30%)** | ND | (Eldar-Finkelman and Martinez, 2011) |
| | 5 | | | → | → | ND | |
| iCRT14 | 50 | 3-catenin-TCF interaction | Inhibits | ↓ **(50%)** | ↓ **(42%)** | → | (Gonsalves et al., 2011) |
| C59 | 15 | Porcupine | Inhibits | ↓ **(43%)** | → | ND | (Proffitt et al., 2013) |
| | 5 | | | → | → | ND | |
| | 1 | | | → | → | ND | |

* The effects were significant when the data from 100 and 20 μM Azakenpaullone- treated explants was pooled

↓ Means that the small molecule reduces the process mentioned compared to controls

↑ Means that the small molecule increases the process mentioned compared to controls

→ Means that the small molecule did not affect the process mentioned compared to controls

The values shown in brackets next to the ↓ and ↑ symbols indicate the percentage of reduction or increase in cell proliferation (BrdU incorporation) or muscle dedifferentiation (SLSs/DAPI ratio) in the treated group compared to the corresponding control group.

ND = Not Determined